CONFIDENTIAL

NACA RM A56K07

UNCLASSIFIED

C.1

3 1176 00094 9587

NACA

RESEARCH MEMORANDUM

A SIMPLIFIED METHOD FOR ASSESSING THE EFFECT OF STEADY ROLLING ON ANGLE OF ATTACK AND SIDESLIP

By Stanley F. Schmidt, Norman R. Bergrun,
Robert B. Merrick, and Howard F. Matthews

Ames Aeronautical Laboratory
Moffett Field, Calif.

CLASSIFICATION CHANGED
UNCLASSIFIED
To [illegible] Date 3/18/60
By authority of TIA # 17

LIBRARY COPY
JAN 29 1957
LANGLEY AERONAUTICAL LABORATORY
LIBRARY, NACA
LANGLEY FIELD, VIRGINIA

CLASSIFIED DOCUMENT

This material contains information affecting the National Defense of the United States within the meaning of the espionage laws, Title 18, U.S.C., Secs. 793 and 794, the transmission or revelation of which in any manner to an unauthorized person is prohibited by law.

NATIONAL ADVISORY COMMITTEE
FOR AERONAUTICS

WASHINGTON

January 17, 1957

CONFIDENTIAL

UNCLASSIFIED

NATIONAL ADVISORY COMMITTEE FOR AERONAUTICS

RESEARCH MEMORANDUM

A SIMPLIFIED METHOD FOR ASSESSING THE EFFECT OF STEADY ROLLING ON ANGLE OF ATTACK AND SIDESLIP

By Stanley F. Schmidt, Norman R. Bergrun,
Robert B. Merrick, and Howard F. Matthews

SUMMARY

Presented herein is a simple method for analyzing the effects of inertia and aerodynamic cross-coupling on the response of airplanes in rolling maneuvers. The method is based on the concept that variations in the calculated steady-state angle of attack and sideslip with roll rate give a measure of the onset and degree of roll coupling. Comparisons are made with the results from five-degree-of-freedom analog-computer studies of unaugmented and augmented airplanes, and it is shown that the method is useful in predicting trends but does not predict magnitudes with sufficient accuracy for loads analysis. Limited flight data are included also to demonstrate the use of the steady-state method in indicating unsatisfactory regions of flight. In addition, the method is shown to be useful in predicting the magnitude of the aileron deflection where serious roll coupling will occur.

INTRODUCTION

Recently, a number of high-speed airplanes have experienced large excursions in angle of attack and sideslip during a rolling maneuver (refs. 1 and 2) which have been attributed to inertia coupling. The possibility of such an occurrence was predicted in 1948 by Phillips in reference 3, wherein he showed that in a steady roll a divergence in yaw and pitch will occur when the rolling frequency approximately equals the uncoupled yawing or pitching natural frequencies. Although Phillips correctly defined the fundamentals of the inertia-coupling phenomenon, the development of a more comprehensive but still simple method for the prediction of serious roll-coupling effects was considered desirable.

The purpose of this paper is to present such a method, referred to as the "steady-state method." This method is based on the concept that the variation of the steady-state angle of attack, sideslip, and other

quantities of interest for various steady rolling velocities gives a measure of the onset and degree of roll coupling. The main substance of this paper, then, includes the derivation of formulas for the steady-state angle of attack, sideslip, etc., from the equations of motion, and an evaluation of this concept by means of a comparison of the steady-state results with analog-computer and flight data.

Prior to the completion of this study, it had come to the authors' attention that others (refs. 4, 5, and 6) had also considered the steady-state approach. However, it is believed that this study treats the problem more extensively and from a somewhat different point of view and therefore should be a useful addition to the expanding literature on the subject.

NOTATION

The analysis made in this report employs a system of body axes. The axis system is shown in figure 1. All angles are in radians unless otherwise noted. A dot above a symbol represents the first derivative with respect to time.

b	wing span, ft
C_Y	lateral-force coefficient, $\frac{\text{lateral force}}{\frac{1}{2}\rho V^2 S}$
C_Z	vertical-force coefficient, $\frac{\text{vertical force}}{\frac{1}{2}\rho V^2 S}$
C_l	rolling-moment coefficient, $\frac{\text{rolling moment}}{\frac{1}{2}\rho V^2 Sb}$
C_m	pitching-moment coefficient, $\frac{\text{pitching moment}}{\frac{1}{2}\rho V^2 S\bar{c}}$
C_n	yawing-moment coefficient, $\frac{\text{yawing moment}}{\frac{1}{2}\rho V^2 Sb}$
$\bar{c}$	mean aerodynamic chord, ft
D	differential operator, $\frac{d}{dt}$

[redacted]

f_α, f_β cyclic frequency in pitch and yaw, respectively, during rolling motion, cps

g acceleration due to gravity, ft/sec^2

G_1, G_2 elevator and rudder servo gains, radians/volt

h_p altitude, ft

I_1 $\frac{I_Z - I_X}{I_Y}$, dimensionless

I_2 $\frac{I_{XZ}}{I_Y}$, dimensionless

I_3 $\frac{I_Y - I_X}{I_Z}$, dimensionless

I_4 $\frac{I_{XZ}}{I_Z}$, dimensionless

I_5 $\frac{I_Z - I_Y}{I_X}$, dimensionless

I_6 $\frac{I_{XZ}}{I_X}$, dimensionless

I_M $\frac{I_{X_e}\omega_e}{I_Y}$, dimensionless $\frac{slug\text{-}ft^2}{slug\text{-}ft^2} \quad \frac{1}{sec}$

I_N $\frac{I_{X_e}\omega_e}{I_Z}$, dimensionless

I_X, I_Y, I_Z moment of inertia in roll, pitch, and yaw, respectively, referred to body axis, $slug\text{-}ft^2$

I_{XZ} product of inertia referred to body axes, $slug\text{-}ft^2$

I_{X_e} polar moment of inertia of jet engine rotating member, $slug\text{-}ft^2$

[redacted]

m	mass of airplane, slugs
M	Mach number
p,q,r	rolling, pitching, and yawing velocities, respectively, radians/sec
p_o	steady rolling velocity, radians/sec
R_φ	roll subsidence root, dimensionless
S	wing area, sq ft
t	time, sec
Δt	incremental time interval, sec
V	free-stream velocity, ft/sec
V_{pr}, V_{pq}, V_q, V_r	voltage proportional to subscript quantity
α	angle of attack
β	angle of sideslip
δ_a	total aileron deflection, positive for trailing edge of right aileron down
i_t	horizontal stabilizer deflection, positive for trailing edge down
Δi_t	horizontal stabilizer deflection above that required for trim
δ_r	rudder deflection, positive for left rudder
ϵ	declination of principal axis below body axis
$\zeta_\alpha, \zeta_\beta$	damping ratio in pitch and yaw, respectively, during rolling motion unless otherwise noted, dimensionless
θ	angle of pitch of longitudinal body axis
ρ	air density, slugs/cu ft
φ	angle of roll

[redacted]

$\Delta\varphi$ incremental angle of roll

ω_e angular velocity of jet engine rotating member, radians/sec; positive rotation is clockwise when viewed from tail of aircraft

Subscripts

av average

ss steady state

crit critical

$C_{Y_\beta}, C_{n_\beta}, C_{m_{\dot{\alpha}}}$ $\left.\begin{matrix}\\\\\end{matrix}\right\}$ $\frac{\partial C_Y}{\partial \beta}, \frac{\partial C_n}{\partial \beta}, \frac{\partial C_m}{\partial \frac{\dot{\alpha}\bar{c}}{2V}}$, . . ., etc.

Derivatives

Y_β, Y, Y_r, Y_p $\frac{\rho VS}{2m}\left(C_{Y_\beta}, C_{Y_{\delta_a}}\delta_a + C_{Y_{\delta_r}}\delta_r, C_{Y_r}\frac{b}{2V}, C_{Y_p}\frac{b}{2V}\right)$

Z_α, Z $\frac{\rho VS}{2m}\left(C_{Z_\alpha}, C_{Z_o} + C_{Z_{i_t}} i_t\right)$ $\frac{\text{slug/ft}^3 \cdot \text{ft/sec} \cdot \text{ft}^2}{\text{slug}} = \frac{1}{\text{sec}}$

Z_g, Y_g $\frac{g}{V}$ $\frac{\text{ft/sec}^2}{\text{ft/sec}} = \frac{1}{\text{sec}}$

$M_\alpha, M_\beta, M_{i_t}, M_{\dot{\alpha}}, M_q$ $\left.\begin{matrix}\\\\\end{matrix}\right\}$ $\frac{\rho V^2 S\bar{c}}{2I_Y}\left(C_{m_\alpha}, C_{m_\beta}, C_{m_o} + C_{m_{i_t}} i_t, C_{m_{i_t}}, C_{m_{\dot{\alpha}}}\frac{\bar{c}}{2V}, C_{m_q}\frac{\bar{c}}{2V}\right) = \frac{\frac{\text{slug}}{\text{ft}^3} \cdot \frac{\text{ft}^2}{\text{sec}^2} \cdot \text{ft}^2 \cdot \text{ft}}{\text{slug} \cdot \text{ft}^2}$

$= \frac{1}{\text{sec}^2}$

$N_\beta, N, N_{\delta_r}, N_{\dot{\beta}}, N_r, N_p$ $\left.\begin{matrix}\\\\\end{matrix}\right\}$ $\frac{\rho V^2 Sb}{2I_Z}\left(C_{n_\beta}, C_{n_{\delta_a}}\delta_a + C_{n_{\delta_r}}\delta_r, C_{n_{\delta_r}}, C_{n_{\dot{\beta}}}\frac{b}{2V}, C_{n_r}\frac{b}{2V}, C_{n_p}\frac{b}{2V}\right)$

[redacted]

$L_\beta, L, L_r, L_p \qquad \frac{\rho V^2 S b}{2 I_X}\left(C_{l_\beta},\ C_{l_{\delta_a}}\delta_a + C_{l_{\delta_r}}\delta_r,\ C_{l_r}\frac{b}{2V},\ C_{l_p}\frac{b}{2V}\right)$

where Y,Z,L,M, and N are total forces or moments at the start of the rolling maneuver.

THE STEADY-STATE METHOD

Illustrated in figure 2 is a typical aircraft angle of attack versus sideslip analog-computer record for an applied constant aileron deflection with rudder and horizontal stabilizer held fixed at their initial trim values. In this instance, the aircraft started its rolling motion from initial trim conditions of 4° angle of attack and zero sideslip and when allowed to roll indefinitely tended to stabilize around a new steady-state condition, denoted in the figure by α_{ss} and β_{ss}. It is the variation of these and other pertinent steady-state values for various constant roll rates and the interpretation thereof that is the basis of the steady-state method which follows.

Derivation of the Steady-State Formulas

For this analysis a constant forward velocity and a constant altitude are assumed. The equations of motion used are the five-degree-of-freedom rigid-body equations. The five equations are:

$$\dot{\beta} + r - p\alpha = Y_\beta \beta + Y_r r + Y_p p + Y_g \cos\theta \sin\varphi + Y \tag{1}$$

$$\dot{\alpha} - q + p\beta = Z_\alpha \alpha + Z_g \cos\theta \cos\varphi + Z \tag{2}$$

$$\dot{q} - I_1 pr + I_2(p^2 - r^2) + I_M r = M_\alpha \alpha + M_{\dot{\alpha}}\dot{\alpha} + M_q q + M_\beta \beta + M \tag{3}$$

$$\dot{r} + I_3 pq + I_4(-\dot{p} + qr) - I_N q = N_\beta \beta + N_{\dot{\beta}}\dot{\beta} + N_r r + N_p p + N \tag{4}$$

$$\dot{p} + I_5 qr - I_6(\dot{r} + pq) = L_\beta \beta + L_p p + L_r r + L \tag{5}$$

There are several different methods[1] for solving these equations to obtain the steady-state values for a constant roll rate ($p = p_o$) and fixed

[1]Another method is to transform equations (1) to (4) directly to algebraic equations by setting $\dot{q} = \dot{r} = \dot{\alpha} = \dot{\beta} = Z = Y_g = 0$ and $p = p_o$. However, this procedure results in an equation which is of greater than the first degree in the particular quantity desired. For example, α_{ss} must be obtained from a cubic algebraic equation of which only one root is of practical significance.

[redacted]

controls. A convenient one, which has the advantage of yielding formulas (in the absence of nonlinear aerodynamic derivatives) that can be used in some instances to easily predict effects of parameter changes, is to linearize equations (1) to (4) by assuming:

$$p = p_o = \text{a constant}$$

$$\varphi = \int p\, dt = p_o t$$

$$r^2 \ll p_o^2$$

$$I_4 q \ll N_r$$

$$\theta \cong 0^\circ$$

The resulting four linear differential equations then can be solved by standard operational techniques to give:

$$(D^4+a_3D^3+a_2D^2+a_1D+a_o)\alpha = b_o+b_1Z_g\sin p_o t+b_2Z_g\cos p_o t$$

$$(D^4+a_3D^3+a_2D^2+a_1D+a_o)\beta = c_o+c_1Y_g\sin p_o t+c_2Y_g\cos p_o t$$

where the a's, b's, and c's are constants and combinations of inertia and aerodynamic parameters and the rolling velocity, p_o. If these fourth-order differential equations are stable and the initial conditions are known, the time solution[2] for α and β will be of the form

$$\alpha(t) = \frac{b_o}{a_o} + \begin{pmatrix}\text{decaying}\\ \text{transients}\end{pmatrix} + \begin{pmatrix}\text{sinusoidal oscillations}\\ \text{due to gravity term } Z_g\end{pmatrix}$$

$$\beta(t) = \frac{c_o}{a_o} + \begin{pmatrix}\text{decaying}\\ \text{transients}\end{pmatrix} + \begin{pmatrix}\text{sinusoidal oscillations}\\ \text{due to gravity term } Y_g\end{pmatrix}$$

or the steady state is

$$\alpha_{ss} = \frac{b_o}{a_o} \tag{6}$$

$$\beta_{ss} = \frac{c_o}{a_o} \tag{7}$$

[2]In reference 7 Sternfield has derived expressions of an approximate time solution for α and β assuming a constant roll rate.

[redacted]

The complete expressions for the constants a_o, b_o, and c_o may be found in Appendix A. The divergent boundary is given by $a_o = 0$. With appropriate simplifications to the terms of a_o, this equation can be reduced to that given by Phillips in reference 3.

To demonstrate certain points in subsequent portions of this report, it is convenient to omit the minor parameters Y, Y_β, Y_p, Y_r, Z, N_p, and M_β in the expressions for a_o, b_o, and c_o. The equations for α_{ss} and β_{ss} then reduce to:

$$\alpha_{ss} = \frac{(I_2p_o^2-M)(I_3p_o^2-I_Np_o-N_\beta)-NM_qp_o}{(I_1p_o^2-I_Mp_o+M_\alpha)(I_3p_o^2-I_Np_o-N_\beta)+M_qN_rp_o^2+M_qZ_\alpha N_\beta} \tag{8}$$

$$\beta_{ss} = \frac{(I_2p_o^2-M)[(I_3Z_\alpha+N_r)p_o-I_NZ_\alpha]+N[I_1p_o^2-I_Mp_o+(M_\alpha-M_qZ_\alpha)]}{(I_1p_o^2-I_Mp_o+M_\alpha)(I_3p_o^2-I_Np_o-N_\beta)+M_qN_rp_o^2+M_qZ_\alpha N_\beta} \tag{9}$$

Although α_{ss} and β_{ss} are perhaps the most important of the steady-state quantities, three other useful relationships can be derived from equations (1), (2), and (5). These are, respectively:

$$r_{ss} = \frac{p_o\alpha_{ss}+Y_\beta\beta_{ss}+Y_pp_o+Y}{1-Y_r}$$

$$q_{ss} = p_o\beta_{ss}-Z_\alpha\alpha_{ss}-Z$$

$$\delta_{a_{ss}} = \frac{I_5q_{ss}r_{ss}-I_8p_oq_{ss}-L_\beta\beta_{ss}-L_rr_{ss}-L_pp_o}{\frac{qSb}{I_X}C_{l_{\delta_a}}} - \frac{C_{l_r}\delta_r}{C_{l_{\delta_a}}} \tag{10}$$

Character of Results

As noted, the equations for the quantities of interest are algebraic equations which are functions of aerodynamic and inertia parameters and the rolling velocity p_o. With known values of the parameters it is

possible to assume various values of p_o and compute the corresponding magnitudes of α_{ss}, β_{ss}, etc. An iteration procedure must be used if $C_{n_{\delta_a}}$ is not zero or if the other aerodynamic derivatives are functions of α or β. An illustrative example of the type of information which is obtained from such computations is given in figure 3. In figure 3(a) are shown three areas of rolling velocity and the basic factors which govern the magnitudes of α_{ss} and β_{ss} in these regions. Of the three, the intermediate range of rolling velocity will be of most interest, since it is here that the largest changes in α_{ss} and β_{ss} occur. As previously mentioned, it is postulated that these changes in magnitude from trim conditions determine the degree of inertia coupling encountered by an aircraft doing aileron rolls with fixed rudder and stabilizer.

Also shown in figure 3(b) are the two distinctly different types of p_o versus $\delta_{a_{ss}}$ plots which can be obtained and which depend primarily on whether favorable or unfavorable yaw occurs. These plots are of importance since they indicate the magnitude of steady rolling velocity the aircraft can achieve. Some interesting points on roll stability will be covered in a subsequent portion of this paper.

EVALUATION OF THE STEADY-STATE CONCEPT

To evaluate the method, the steady-state solutions were compared with the results of analog-computer studies and with flight data. Although these comparisons showed that it was not possible to predict the peak magnitudes of the transient α and β with sufficient accuracy for loads analysis, the steady-state solution did correctly indicate the onset and severity of roll coupling. A few selected examples follow to illustrate the degree of comparison and the usefulness of the steady-state concept.

The characteristics of the F-100A and the F-102A airplanes were used in the calculations and a summary of their mass, geometric, and aerodynamic properties is given in tables I and II. However, unless otherwise noted, the basic characteristics of the large-tail F-100A airplane at $M = 0.7$ and 30,000 feet with $C_{n_{\delta_a}} = 0$ were used in the following comparisons and will be identified in the text as the "example aircraft." The steady-state α and β were computed from the complete equations (6) and (7) unless otherwise noted.

Comparison of the Steady-State With Analog-Computer Results

Throughout this section of the report, five-degree-of-freedom ($\dot{V} = 0$) analog-computer results are presented for approximate 360° aileron rolls.

These 360° rolls are made with pilot applied fixed elevator (or stabilizer) and no rudder input during the roll. In figure 4 are shown typical records for such a roll with the maximum excursions and average roll rate indicated. On subsequent figures the maximum excursions in sideslip and in angle of attack plus the trim α are used for the comparison with the results of the steady-state method.

Relationship of pitching and yawing frequencies.- References 3, 8, and others have shown that it is desirable to have the pitching and yawing frequencies of the aircraft equal or close to each other. This conclusion is drawn from a study of the equation defining the divergent boundaries, $a_o = 0$, as follows:

Consider the denominator a_o of the simplified expression for α_{ss} or β_{ss} (eq. (8) or (9)),

$$(\overset{+}{I_1}p_o^2-\overset{+}{I_M}p_o+\overset{-}{M_\alpha})(\overset{+}{I_s}p_o^2-\overset{+}{I_N}p_o-\overset{+}{N_\beta})+\overbrace{M_qN_rp_o^2}^{+}+\overbrace{M_qZ_\alpha N_\beta}^{+} \tag{11}$$

Now when the normal signs shown above the parameters are examined, it is seen that a_o will always remain positive (and therefore stable) if the bracketted terms reverse sign at the same rolling velocity. The relationship of the parameters which are necessary for this reversal is seen to be:

$$\left.\begin{aligned} &\frac{I_1}{I_s} = \frac{I_M}{I_N} = \frac{M_\alpha}{-N_\beta} \\ \text{or} \quad &\frac{\dfrac{I_Z-I_X}{I_Y}}{\dfrac{I_Y-I_X}{I_Z}} = \frac{\dfrac{I_{X_e}\omega_e}{I_Y}}{\dfrac{I_{X_e}\omega_e}{I_Z}} = \frac{M_\alpha}{-N_\beta} \end{aligned}\right\} \tag{12}$$

The only manner in which the above relationship can be realized is for $I_Y = I_Z$ and $M_\alpha = -N_\beta$, the latter being the equality between the square of the pitching natural frequency and the square of the yawing natural frequency. Since I_Z is always larger than I_Y, the foregoing relationship can be approached but not exactly achieved.

For later use, the rates of roll at which either of the bracketted terms in equation (11) become zero are defined as critical rolling velocities. They are:

$$p_{crit_\alpha} = \frac{I_M \pm \sqrt{I_M^2 - 4M_\alpha I_1}}{2I_1} \cong \frac{I_{X_e}\omega_e}{2(I_Z - I_X)} \pm \sqrt{\frac{-M_\alpha}{\frac{I_Z - I_X}{I_Y}}} \tag{13}$$

$$p_{crit_\beta} = \frac{I_N \pm \sqrt{I_N^2 + 4N_\beta I_3}}{2I_3} \cong \frac{I_{X_e}\omega_e}{2(I_Y - I_X)} \pm \sqrt{\frac{N_\beta}{\frac{I_Y - I_X}{I_Z}}} \tag{14}$$

Analysis has indicated that when the vertical tail size (i.e., C_{n_β}) of an airplane is proportioned so as to approximate the best relationship between M_α and N_β (eq. (12)), excursions in α and β are alleviated considerably. Since these results also agree with flight experience, it is therefore of interest to examine the effect of arbitrary variations in natural frequency parameters M_α and N_β on the steady-state excursions in α and β, and to compare them with analog-computer results. Figure 5 is presented for discussing the trends which may be expected. Three curves have been calculated for both α_{ss} and β_{ss} using constants and derivatives of the example aircraft, except as noted, starting from trimmed level flight. One curve, shown by the solid line, is for the best value of N_β defined by equation (12) corresponding to the existing value of M_α for the airplane. For this case, $N_\beta = -0.75\ M_\alpha$ and the corresponding value of C_{n_β} is about 15 percent larger than the value tabulated in table I for the large-tail airplane. When N_β is reduced below the best value relative to M_α, α and β excursions are increased. In fact, if N_β is sufficiently small, instability occurs, as can be seen from the dashed curve in figure 5. The dashed curve, identified as N_β being equal to 3/10 of the best value relative to M_α, can be associated with the small-tailed F-100A airplane at the same flight condition. The remaining curve does not represent a particular configuration of the F-100A airplane, but is included to show the effect of increasing N_β and M_α by a factor of 3, at the same time retaining the best relationship between these quantities. Also indicated on the figure for the solid and dashed curves are the critical roll rates obtained from equations (13) and (14). The critical roll rates for the dash-dot curve are out of the range shown.

[redacted]

The data of figure 5 clearly show that large roll coupling can occur when the best relationship formula between N_β and M_α is not observed as well as the beneficial effects of increasing both the natural frequencies in yaw and pitch.

In figure 6, the three curves of figure 5 are compared with results from five-degree-of-freedom analog-computer solutions. The comparison is made in figure 6(a) for the case of N_β having the best value with respect to M_α; in figure 6(b) for $N_\beta = 0.3$ of the best value; and in figure 6(c) for a threefold increase in both N_β and M_α while the best-value relationship is retained. In each of figures 6(a), 6(b), and 6(c), three curves are shown. The solid line is the calculated steady state, the dashed line is the maximum transient excursion for a 360° roll occurring during the departure from trim, and the dash-dot line is the maximum transient excursion during the return to trim. With the single exception of β_{ss} magnitudes at high roll rates (-167° to -195° per second) for the case of $N_\beta = -0.3\ M_\alpha(I_3/I_1)$ in figure 6(b), the magnitudes of the maximum α and β transients during the departure from trim follow the trends predicted by the steady-state equations; those during the return to trim, of course, have no steady-state counterpart. It is apparent, however, that at roll rates less then the lower of the two critical roll rates these transients appear to deviate from the steady-state curve by roughly the same amount as the departure transients, but in an opposite sense. Above this critical roll rate, the return transients follow no obvious pattern with respect to the steady-state values. Thus the trends of the maximum angle of attack and sideslip as affected by roll rate are correctly given by the steady-state method, but the prediction of the magnitudes of these quantities with sufficient accuracy for loads analysis is not possible.

In figure 6(b) (and some subsequent figures) is noted a region in which the airplane continued to roll even though the aileron deflection was reduced to zero. This phenomenon is associated with favorable yaw and possibly could be avoided if the aileron were completely reversed rather than returned to neutral.

Effects of initial angle of attack and elevator deflection.- Previous studies (ref. 8) have shown that the initial angle of attack at the onset of rolling and inadvertent elevator inputs during a roll can have a large influence on the magnitude of the α and β excursions during a rolling maneuver. It is known further that the excursions will be near a minimum if the initial angle of attack is such that the principal axis and flight path are aligned. These effects can be demonstrated also by the use of the steady-state method in the following manner.

In figure 7 are plotted the α_{ss} and β_{ss} for initial angles of attack of -4°, +1°, and +6° for the example aircraft which correspond to initial angles between the principal axis and the flight path of -5°, 0°, and +5°, respectively. As can be noted from the figure, large deviations in α_{ss}

and β_{ss} occur in the region of -80° to -180° per second roll rate for the two cases where the principal axis and flight path are not aligned. Also of interest is the reversal of α_{ss} for roll rates greater than -120° per second. Since the amount of elevator deflection is directly associated with the initial angle of attack, this change would appear to a pilot rolling in this region as a control reversal. The large difference in the extremes of α_{ss} also indicates that the elevator control will be sensitive in this region. Such characteristics have been observed in flight.

Figures 8(a), 8(b), and 8(c) have been prepared to show the comparison between the steady-state values and the analog-computer results. As is seen from these data, the steady-state method is useful in predicting the effects of changes in initial angle of attack.

As an interesting sidelight, the fact that the minimum change in α_{ss} occurs when the principal axis and flight path are nearly aligned can be shown easily from the simplified steady-state equation for α_{ss} as follows:

If the damping and engine inertia terms are neglected, the equation for α_{ss} becomes

$$\alpha_{ss} = \frac{I_2 p_o^2 - M}{I_1 p_o^2 + M_\alpha} = \frac{M}{-M_\alpha} \frac{\left(\frac{1}{M}\frac{I_{XZ}}{I_Y} p_o^2 - 1\right)}{\left(\frac{1}{-M_\alpha}\frac{I_Z - I_X}{I_Y} p_o^2 - 1\right)}$$

When $p_o = 0$ in this equation, $\alpha_{ss} = \alpha_{trim} = M/-M_\alpha$. In order then to maintain $\alpha_{ss} = M/-M_\alpha$ invariant with roll velocity the terms within the parentheses must be equal, or

$$\frac{1}{M}\frac{I_{XZ}}{I_Y} p_o^2 - 1 = \frac{1}{-M_\alpha}\frac{I_Z - I_X}{I_Y} p_o^2 - 1$$

This equality reduces to

$$\frac{M}{-M_\alpha} - \frac{I_{XZ}}{I_Z - I_X} = 0$$

Since by definition $I_{XZ}/(I_Z - I_X)$ is the declination of the principal axis below the body axis, ϵ, the above equation means that if the angle

[redacted]

of attack of the principal axis is zero, no deviation in α_{ss} with p_o will occur. This conclusion, of course, is modified slightly if all the terms affecting α_{ss} are considered.

Augmentation devices.- The use of augmenters to reduce the roll-coupling tendencies of an aircraft has received considerable attention recently (refs. 9 and 10). The purpose here is to demonstrate that the steady-state method provides a means of estimating the effectiveness of an augmenter and the magnitude of the control required. Two devices have been selected for study; one, the artificial damper in yaw or pitch, and the other, a pq plus a pr feedback which tends to cancel certain important inertia-coupling terms in the yawing and pitching equations of motion, respectively. A simplified block diagram of their mechanization for study of five-degree-of-freedom simulation is shown in figure 9.

Artificial dampers: Some analog-computer studies (ref. 8) have indicated that an increase in pitch damping is more effective than an equivalent increase in yaw damping in reducing inertia coupling in a rolling maneuver. A scrutiny of the simplified steady-state equations for α_{ss} and β_{ss} shows that this conclusion should always be true in the absence of yawing moments applied by the aileron or rudder ($N = 0$). For example, increases in pitch and yaw damping by artificial means may be approximated in the steady-state equations by increasing the parameters M_q and N_r, respectively. Referring to equations (8) and (9) and letting N be zero, one sees that M_q occurs twice and only in the denominator, whereas N_r occurs but once in both denominators and in the numerator of β_{ss}. Since increases in M_q or N_r increase the denominator or numerators if the aircraft has not exceeded the divergent boundary, it is apparent that increased M_q (pitch damping) will be more effective than N_r (yaw damping) in reducing either β_{ss} or α_{ss}. This anomaly is confirmed by the data shown in figure 10, on which have been plotted α_{ss} and β_{ss} for the normal example aircraft and for separate increases in the damping in pitch and yaw. The increases in the damping ratios noted were computed from two-degree-of-freedom analyses in pitch and in yaw at zero roll rate and the changes in magnitude were made by appropriate increases in M_q and N_r (ΔM_q, ΔN_r) in the steady-state equations. Also shown in the figure are the steady-state rudder and stabilizer deflections necessary for the augmentation as obtained from the following equations:

$$\delta_{r_{ss}} = \frac{\Delta N_r}{N_{\delta_r}} r_{ss} \qquad \Delta i_{t_{ss}} = \frac{\Delta M_q}{M i_t} q_{ss}$$

The large difference in the deflections of the control surfaces is due primarily to the differences in the control effectiveness. To illustrate that the steady-state method will indicate the effect of artificial dampers

[redacted]

on roll coupling, figures 11(a), 11(b), and 11(c) have been prepared. The data in these figures show a good correspondence, trendwise, between the steady-state and analog-computer results. For the analog simulation the feedback loops C and D of figure 9 were used, with the gains G_1 and G_2 adjusted to give the required damping ratios.

The pq,pr augmenter: It has been shown that an aircraft experiences small roll-coupling effects if it rolls at rates well below the critical roll velocities defined in equations (13) and (14). One means then of reducing such effects is to increase the critical roll rates by the use of an augmenter. As can be seen from the equations defining these critical rates, they may be increased in the limit to infinity by canceling, with pr and pq feedback, the inertia-coupling terms $-I_1pr$ and I_3pq in the pitching and yawing equations of motion, respectively (see refs. 9 and 10 for previous studies on this type augmenter). Figure 12 illustrates the effect of this cancellation on certain steady-state quantities. The steady-state rudder and horizontal stabilizer deflections necessary for the augmentation were computed from the formulas

$$\Delta i_{t_{ss}} = -\frac{\left(\frac{I_Z-I_X}{I_Y}\right)}{Mi_t} p_o r_{ss} \qquad \Delta\delta_{r_{ss}} = \frac{\left(\frac{I_Y-I_X}{I_Z}\right)}{N_{\delta_r}} p_o q_{ss}$$

As can be seen from the data in the figure, the pq,pr feedback device results in a significant decrease in α_{ss} and β_{ss}, but the $\delta_{r_{ss}}$ necessary to achieve these improvements is large. In an effort to reduce the $\delta_{r_{ss}}$ and still retain the desired small variation of α_{ss} and β_{ss} with p_o, artificial damping was added with the favorable results shown in figure 13.

Figure 9, loops A and B, illustrates the method of simulating the pq,pr device on the analog computer. In a practical case the products of pr and pq can be obtained by driving the primaries of two transducers on the roll rate gyro with amplified signals from the yaw and pitch rate gyros. For the analog simulation the gains G_1 and G_2 were adjusted to give exact cancellation of the inertia-coupling terms when the dynamics of the servo were neglected. Figure 14 shows the comparison of the steady-state and the five-degree-of-freedom analog-computer solutions for the two types of augmenters. In general, the data in figure 14 along with that of figure 11(a) show that the steady-state method can be used in a qualitative manner to assess the roll-coupling effects of these special types of stability augmenters.

[redacted]

Ability of the ailerons to create rolling velocity.- Since roll rate has been recognized as a fundamental parameter in the inertia-coupling phenomenon, the foregoing evaluation of the steady-state method has been predicated on a comparison of the calculated steady-state α and β as a function of roll rate with solutions from the five-degree-of-freedom analog simulation. However, it is of importance also in the evaluation to determine the degree to which the steady-state approach can estimate the ability of the aileron to create rolling velocity. In figure 15 are shown such rolling performance data. The corresponding comparisons of α and β have been given in figure 11(a).

The data shown in figure 15 are interesting for several reasons. First, the steady-state solution is seen to have a lower and an upper statically stable branch (solid lines) connected by a statically unstable branch (dash line). Second, is the close correlation in magnitude between the analog-computer results and those of the lower steady-state branch up to about 17° control deflection and the good agreement in trend with the upper stable steady-state branch above 30° aileron deflection. Plotted also in the figure is the straight line of the single degree of freedom relationship between p_o and $\delta_{a_{ss}}$. The difference between the straight-line and the steady-state solution is due primarily to rolling moments induced by sideslip.

During the course of obtaining the analog-computer data, some runs were made for rolls greater than 360°. These data matched the steady-state lower branch closely up to a δ_a of about 25° at which point a jump in roll rate occurred so that for larger control deflections the steady-state upper branch was followed. Some understanding of the reason for this discontinuity in the roll rate was obtained by considering small perturbations about the steady-state values and solving for the characteristic modes of the five equations of motion. The method of reference 6 was used but only the most important derivatives and inertia terms were retained for these small-perturbation computations (I_2, I_4, I_6, Y_β, Y_p, Y_r, $M_{\dot{\alpha}}$, M_β, $N_{\dot{\beta}}$, N_p, and L_r were set equal to zero). The results are given in figure 16 for the lower statically stable steady-state branch. These data show that the yaw or dutch roll mode becomes dynamically unstable at 27° control deflection. Whether this good agreement between the perturbation analysis and the analog-computer results will occur for different aerodynamic derivatives is not known, as transient effects are important in determining the critical aileron deflection.

Since it has been noted by others that the derivative $C_{n_{\delta_a}}$ has some influence on the roll-coupling problem, the steady-state solutions were computed to illustrate the effect of a change in this derivative at both a subsonic and a supersonic speed. These results are given in figure 17 and show that a favorable yawing moment due to control deflection tends to add favorable yaw (or reduce unfavorable yaw) for the lower

branch at either Mach number and so increase the roll rate for a given aileron deflection. This effect is so pronounced at the supersonic speed that the steady-state solution becomes statically unstable at a roll rate of -190° per second with a moderate amount of favorable yawing moment. The stability in this instance was checked also by the perturbation technique at roll rates of -190° and -210° per second. The results of these computations are noted in figure 17 and show that at the lower roll rate the roll subsidence root is convergent but at -210° per second it is divergent.

The usefulness of the steady-state method and the perturbation technique for determining the ability of the aileron to create rolling velocity is that it offers a means of assessing the areas of aileron deflection (or roll rate) where serious roll coupling occurs. Thus, it offers a way of judging where to limit the control deflection (or roll rate) if this means is used to avoid roll-coupling difficulties.

Comparison of Steady-State Solution With Pilot Opinion

The main objective of the steady-state approach is to provide a simple qualitative method whereby in preliminary design one can quickly assess the onset and degree of roll-coupling effects for any selected flight condition. The method would be of questionable value, however, if its results were in conflict with pilot opinion regarding actual airplane performance. Some unpublished pilot-opinion data have been obtained from the NACA High-Speed Flight Station at Edwards Air Force Base, California. These data, which are for 360° rudder-fixed aileron rolls, are compared with steady-state solutions in figure 18. Three categories of pilot acceptability are shown: intolerable (fig. 18(a)); good (fig. 18(b)); and marginal (fig. 18(c)).

In the "intolerable" plot (fig. 18(a)) are the F-102A airplane at one flight condition (curve A) and the F-100A small-tail airplane at two flight conditions (curves B and C). These "intolerable" experiences are all characterized by having excessively large calculated steady-state β excursions over a sizable roll-rate region attainable by the airplane. The good flight experience (fig. 18(b)) have been with the large-tail F-100A airplane at two high-speed flight conditions (M = 1.20 and 1.26), and are shown by curves D and E in the figure. These good experiences are characterized by small steady-state excursions in the roll-rate region attainable. The short vertical lines intersecting the calculated steady-state curves designate the average roll rate experienced during the particular flight test. For the two conditions shown, these roll rates are well below the critical rolling frequency. The marginal experiences (fig. 18(c)) have been with the large-tail F-100A airplane at three subsonic flight conditions (M = 0.70 and 0.93 and altitudes of 30,000 and 40,000 feet). Here, the excursions are relatively large (curves F

and G), but these do not cover a broad range of roll rates in the roll-rate region attainable by the airplane. It should be noted that for curve G, the roll rate experienced was above the critical. For the flight condition at $M = 0.93$ at 40,000 feet (curve H), the maximum roll rate experienced during the maneuver was on the border of the critical roll-rate region. For this condition, the pilot was able to detect an impending undesirable condition and so evaluated the flight experience as marginal.

In summary, one can conclude that pilot opinion is consistent with the steady-state concept in these important respects; all divergent conditions given by steady-state calculations and within the rolling capabilities of the aircraft have been recognized as unacceptable by the pilots; all good conditions have been those experienced at high speeds where the critical rolling frequencies are high, and at roll rates which have been appreciably below these critical frequencies. All marginally acceptable conditions have been those in which roll rate either has remained just below the critical regime or has passed unobtrusively through it.

These marginal cases could very well become unacceptable for roll maneuvers initiated from initial conditions other than those shown, since the aircraft is rolling at rates in the critical region where initial angle of attack, inadvertent elevator motions, and other effects can cause an appreciable change in the magnitude of the actual excursion from trim.

CONCLUSIONS

An analytical method has been developed herein for use in analyzing the roll-coupling phenomenon. This method is based on the concept that variations in the calculated steady-state angle of attack and sideslip with roll rate give a measure of the onset and degree of roll coupling. From the results of comparisons of the steady-state values with those from five-degree-of-freedom analog-computer studies and from limited flight data the following conclusions are drawn:

1. The trends of the maximum angles of attack and sideslip as affected by roll rate are correctly given by the steady-state method, but the prediction of the magnitudes of these quantities with sufficient accuracy for loads analysis is not possible.

2. An analysis of the steady-state equations provides an understanding of and a useful guide for determining the effects of various aerodynamic and inertia parameters on roll coupling.

3. The method appears useful to define critical flight conditions and to assess the merits of various stability augmenters devised to minimize roll-coupling effects.

[redacted]

4. The method, because of the ease and rapidity with which calculations can be made, appears particularly promising for preliminary design work in defining areas in which a complete simulator study should be undertaken.

Ames Aeronautical Laboratory
National Advisory Committee for Aeronautics
Moffett Field, Calif., Nov. 7, 1956

[redacted]

APPENDIX A

THE COMPLETE COEFFICIENTS OF THE STEADY-STATE SOLUTION FOR α_{ss} AND β_{ss}

The constants a_o, b_o, and c_o of equations (6) and (7) are:

$$a_o = I_1I_3p_o^4+(-I_MI_3-I_NI_1)p_o^3+[(1-Y_r)I_3M_\alpha-I_1N_\beta+M_qN_r+I_MI_N+I_1I_3Y_\beta Z_\alpha]p_o^2+$$
$$[(1-Y_r)(I_3M_\beta Z_\alpha-I_NM_\alpha)+I_MN_\beta-Z_\alpha Y_\beta(I_1I_N+I_3I_M)+M_\beta N_r]p_o+$$
$$\left\{[(1-Y_r)N_\beta+N_rY_\beta](-M_\alpha+M_qZ_\alpha)+I_NZ_\alpha[I_MY_\beta-(1-Y_r)M_\beta]\right\}$$

$$b_o = [I_2I_3(1-Y_r)-I_1I_3Y_p]p_o^4+[-I_2I_N(1-Y_r)-I_1I_3Y+Y_p(I_1I_N+I_3I_M)]p_o^3+$$
$$[(1-Y_r)(-I_3M-I_2N_\beta-M_qN_p)+Y(I_1I_N+I_3I_M)+Y_p(I_1N_\beta-I_MI_N-M_qN_r)+$$
$$Y_\beta(-I_2N_r-I_1N_p-I_1I_3Z)]p_o^2+[(1-Y_r)(MI_N-NM_q-I_3ZM_\beta-N_pM_\beta)+Y(I_1N_\beta-I_MI_N-M_qN_r)+$$
$$Y_p(-I_MN_\beta-N_rM_\beta)+Y_\beta(-I_1N+I_1I_NZ+I_3I_MZ+I_MN_p)]p_o+[(1-Y_r)(MN_\beta-M_qZN_\beta+I_NM_\beta Z-$$
$$NM_\beta)+Y(-I_MN_\beta-N_rM_\beta)+Y_\beta(MN_r-M_qZN_r-I_MI_NZ+I_MN)]$$

$$c_o = \left\{[I_2I_3(1-Y_r)-I_1I_3Y_p]Z_\alpha+I_1(I_3Z+N_p)+I_2N_r\right\}p_o^3+\left\{[-I_2I_N(1-Y_r)-I_1I_3Y+\right.$$
$$\left.Y_p(I_1I_N+I_3I_M)]Z_\alpha-I_M(I_3Z+N_p)+I_1(N-I_NZ)\right\}p_o^2+[(1-Y_r)(-I_3MZ_\alpha+M_\alpha N_p+I_3M_\alpha Z-$$
$$M_qZ_\alpha N_p)+Z_\alpha Y(I_1I_N+I_3I_M)+Y_p(-I_MI_NZ_\alpha-M_qN_rZ_\alpha+M_\alpha N_r)-(MN_r-M_qZN_r-I_MI_NZ+$$
$$I_MN)]p_o+[(1-Y_r)(NM_\alpha-M_qZ_\alpha N+I_NMZ_\alpha-I_NM_\alpha Z)+Y(-I_MI_NZ_\alpha-M_qN_rZ_\alpha+M_\alpha N_r)]$$

[redacted]

REFERENCES

1. NACA High-Speed Flight Station: Flight Experience With Two High-Speed Airplanes Having Violent Lateral-Longitudinal Coupling in Aileron Rolls. NACA RM H55A13, 1955.

2. Finch, T. W., Peele, J. R., and Day, R. E.: Flight Investigation of the Effect of Vertical-Tail Size on the Rolling Behavior of a Swept-Wing Airplane Having Lateral-Longitudinal Coupling. NACA RM H55L28a, 1955.

3. Phillips, William H.: Effect of Steady Rolling on Longitudinal and Directional Stability. NACA TN 1627, 1948.

4. Uddenberg, R. C., et al: The Dynamic Stability and Control Equations of a Pivoted-Wing Supersonic Pilotless Aircraft, With Downwash, Wake and Interference Effects Included. Document D-8510, Boeing Airplane Co., 1948.

5. Pinsker, W. J. G.: Preliminary Note on the Effect of Inertia Cross-Coupling on Aircraft Response in Rolling Manoeuvres. R.A.E. TN No. Aero 2419, Ministry of Supply, Nov. 1955.

6. Kelley, H. J., Hinz, H. K., and Kress, R. W.: Grumman Experience With Aerodynamic and Inertial Cross-Coupling Effects in Rolling Maneuvers. Grumman Aircraft Engr. Corp., Mar. 1, 1956.

7. Sternfield, Leonard: A Simplified Method for Approximating the Transient Motion in Angles of Attack and Sideslip During a Constant Rolling Maneuver. NACA RM L56F04, 1956.

8. Weil, Joseph, and Day, R. E.: An Analog Study of the Relative Importance of Various Factors Affecting Roll Coupling. NACA RM H56A06, 1956.

9. Creer, Brent Y.: An Analog Computer Study of Several Stability Augmentation Schemes Designed to Alleviate Roll-Induced Instability. NACA RM A56H30, 1956.

10. Phillips, William H.: Analysis of an Automatic Control to Prevent Rolling Divergence. NACA RM L56A04, 1956.

[redacted]

TABLE I.- SUMMARY OF PHYSICAL PROPERTIES AND DERIVATIVES FOR THE F-100A AIRPLANE
[All derivatives not listed are taken as zero]

Physical Properties

$\bar{c}$	11.33	I_X	11,050	I_{XZ}	508
b	36.58	I_Y	59,000	$I_{X_e}\omega_e$	17,550
S	376.0	I_Z	67,000	m	745

Derivatives

	M = 0.64	M = 0.70	M = 0.93	M = 1.20	M = 1.26
C_{Z_α}	-3.89	-4.27	-4.87	-3.84	-3.84
$C_{m_{i_t}}$	---	-1.00	---	-.60	---
C_{m_q}	-3.60	-3.75	-5.55	-4.15	-4.15
C_{m_α}	-.29	-.42	-.81	-1.22	-.91
$C_{m_{\dot{\alpha}}}$	---	-1.25	---	-1.35	---
C_{n_p}	0	-.025	0	0	0
C_{n_r}	-.16	-.30	-.29	-.19	-.19
C_{n_β} (large tail)	---	.095	.109	.097	.086
C_{n_β} (small tail)	.039	.043	---	---	---
$C_{n_{\delta_a}}$	---	-.006	---	-.0095	---
$C_{n_{\delta_r}}$	---	-.0315	---	---	---
C_{Y_p}	0	.17	0	0	0
C_{Y_r}	0	.34	0	0	0
C_{Y_β}	0	-.62	0	0	0
C_{l_p}	---	-.29	---	-.406	---
C_{l_r}	---	.12	---	.03	---
C_{l_β} at $\alpha = 0$	---	-.008	---	-.050	---
$\partial C_{l_\beta}/\partial\alpha$	---	-.516	---	-.332	---
$C_{l_{\delta_a}}$	---	-.044	---	-.038	---

[redacted]

TABLE II.- SUMMARY OF PHYSICAL PROPERTIES AND DERIVATIVES
FOR THE F-102A AIRPLANE AT M = 0.75
[All derivatives not listed are taken as zero]

Physical Properties

$\bar{c}$	23.1	I_X	13,600	I_{XZ}	2310
b	37.8	I_Y	89,400	$I_{X_e}\omega_e$	17,550
S	661.5	I_Z	99,600	m	711

Derivatives

C_{Z_α}	-2.81
C_{m_q}	-1.20
C_{m_α}	-.258
C_{n_r}	-.069
C_{n_β}	.065

[redacted]

[redacted]

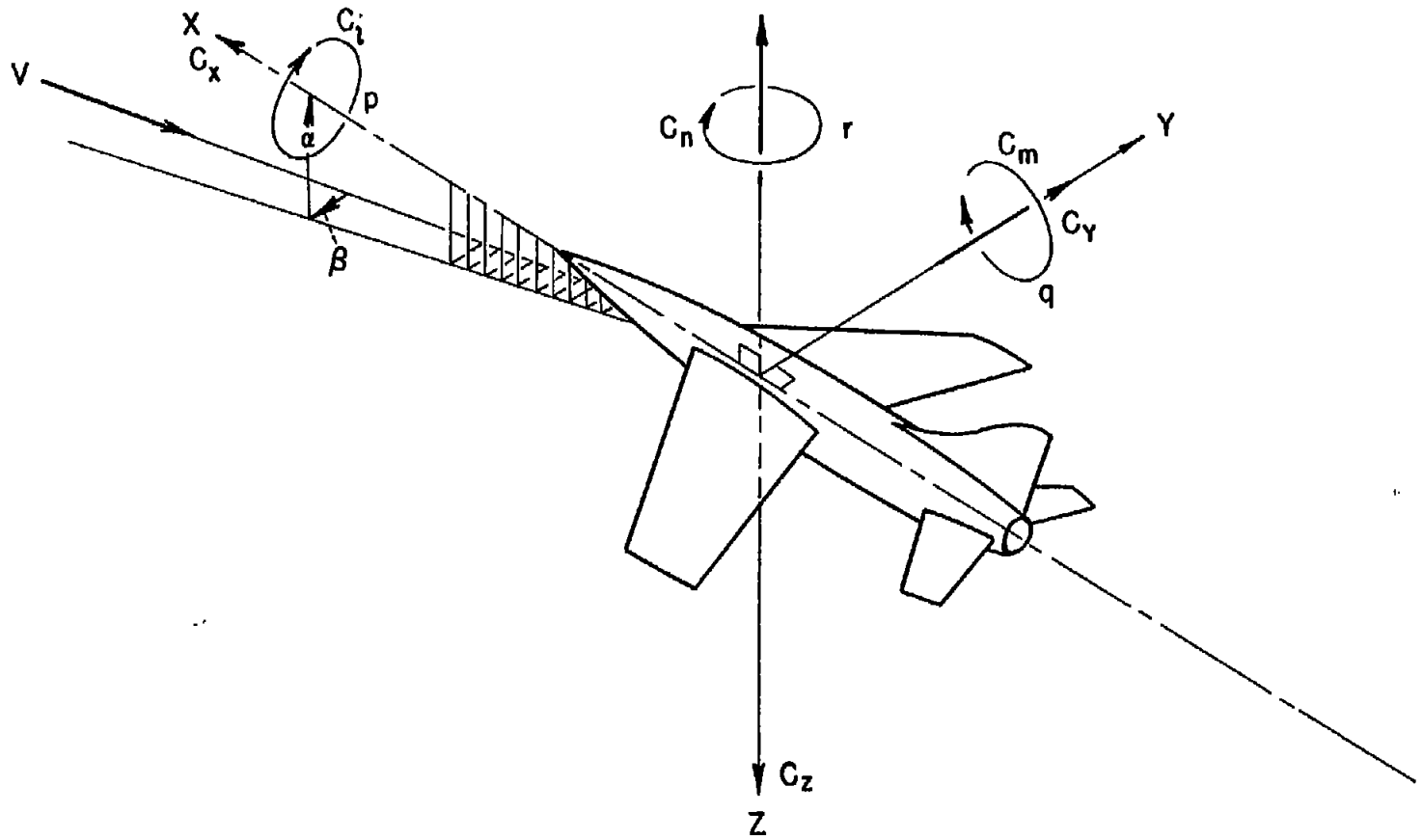

Figure 1.- System of axes (positive values of forces, moments, and angles are indicated by arrows).

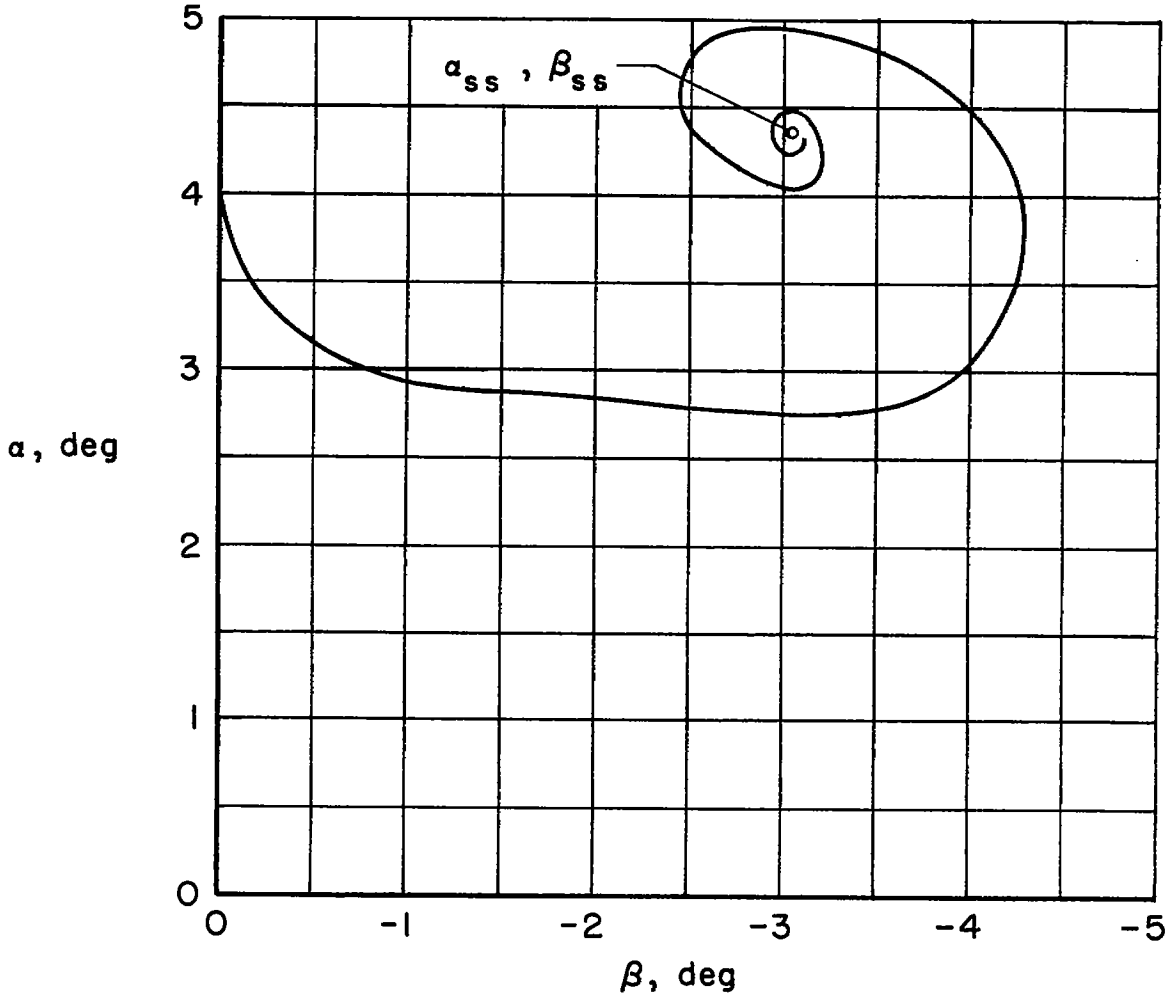

Figure 2.- Typical response of α and β to an applied aileron deflection; gravity terms omitted.

[redacted]

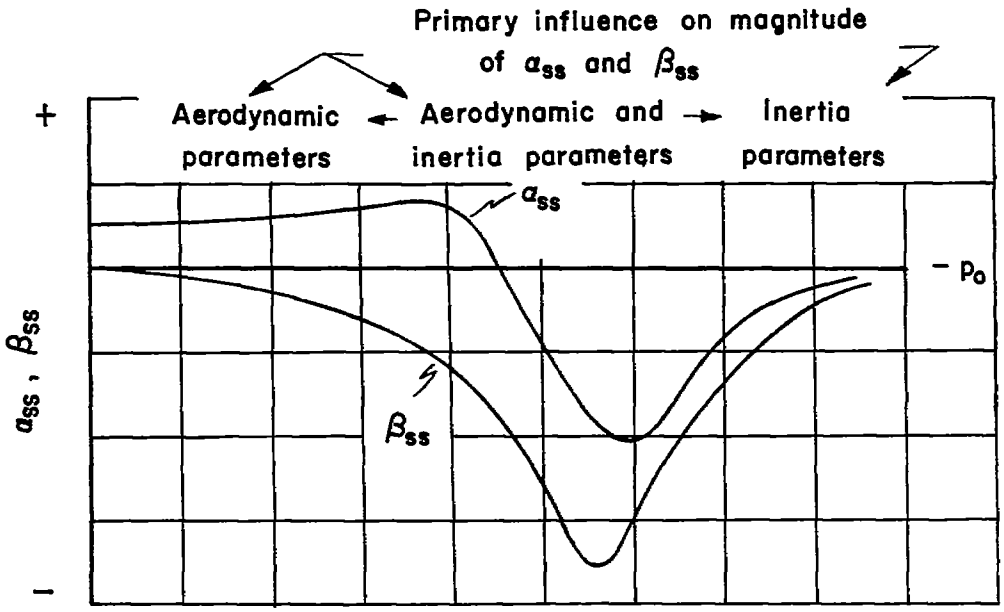

(a) Illustrative α_{ss} and β_{ss} vs. p_o results.

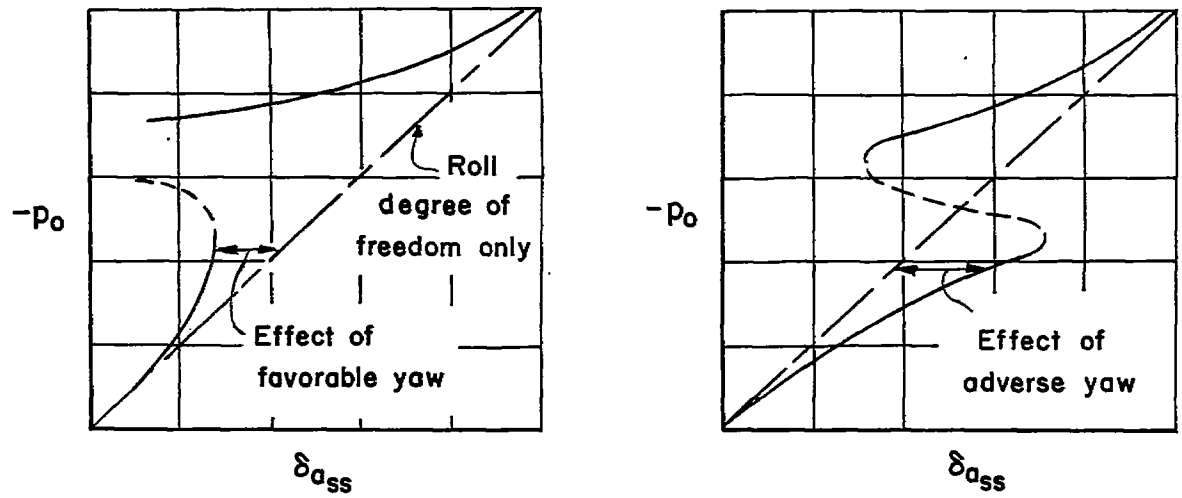

(b) Illustrative p_o vs. $\delta_{a_{ss}}$ results.

Figure 3.- Character of results of steady-state computations.

[redacted]

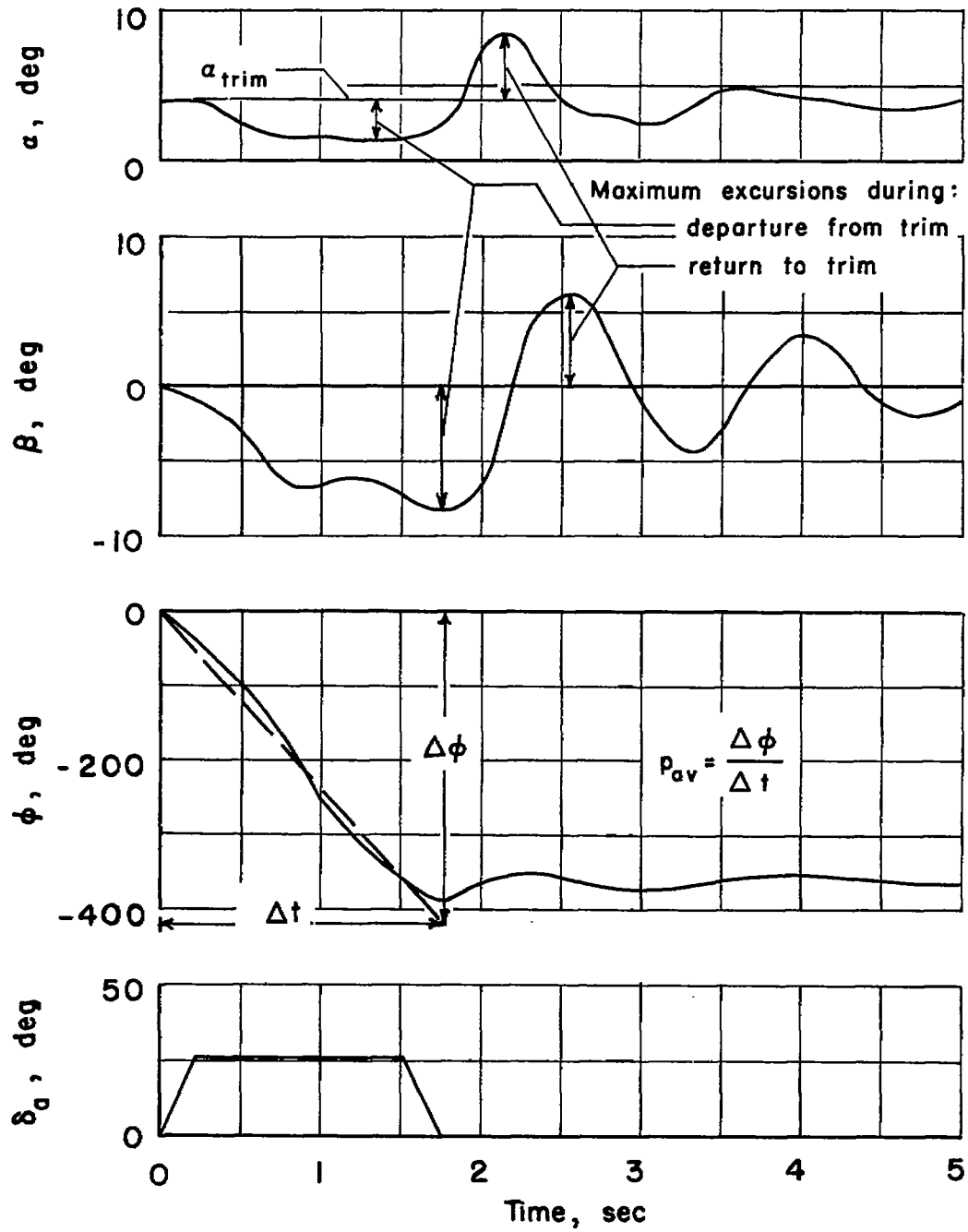

Figure 4.- Time histories of typical 360° roll maneuver showing values of α and β used for comparing five-degree-of-freedom analog-computer results with steady-state calculations.

[redacted]

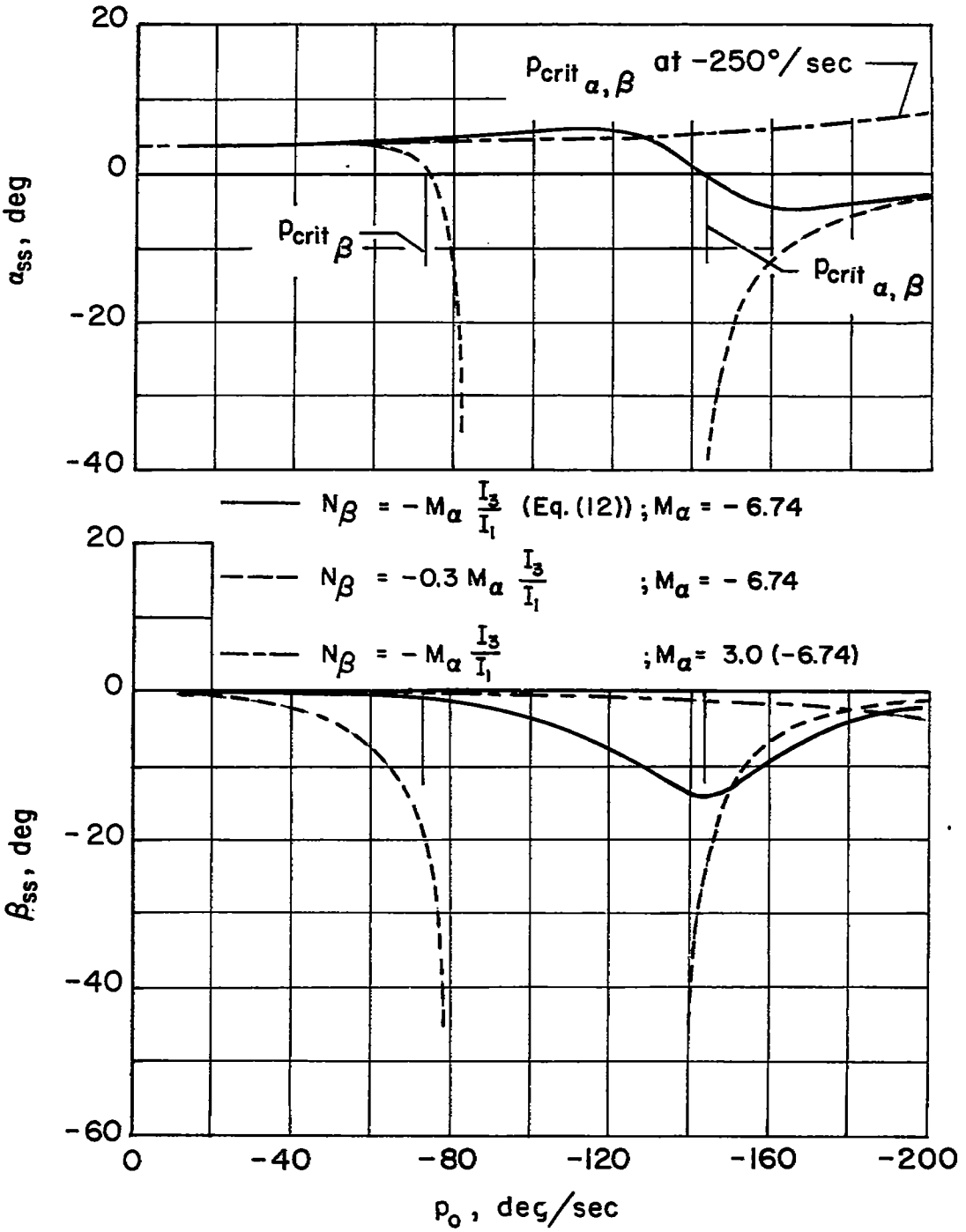

Figure 5.- Characteristic trends in α_{ss} and β_{ss} due to changes in the airplane frequency parameters M_α and N_β.

[redacted]

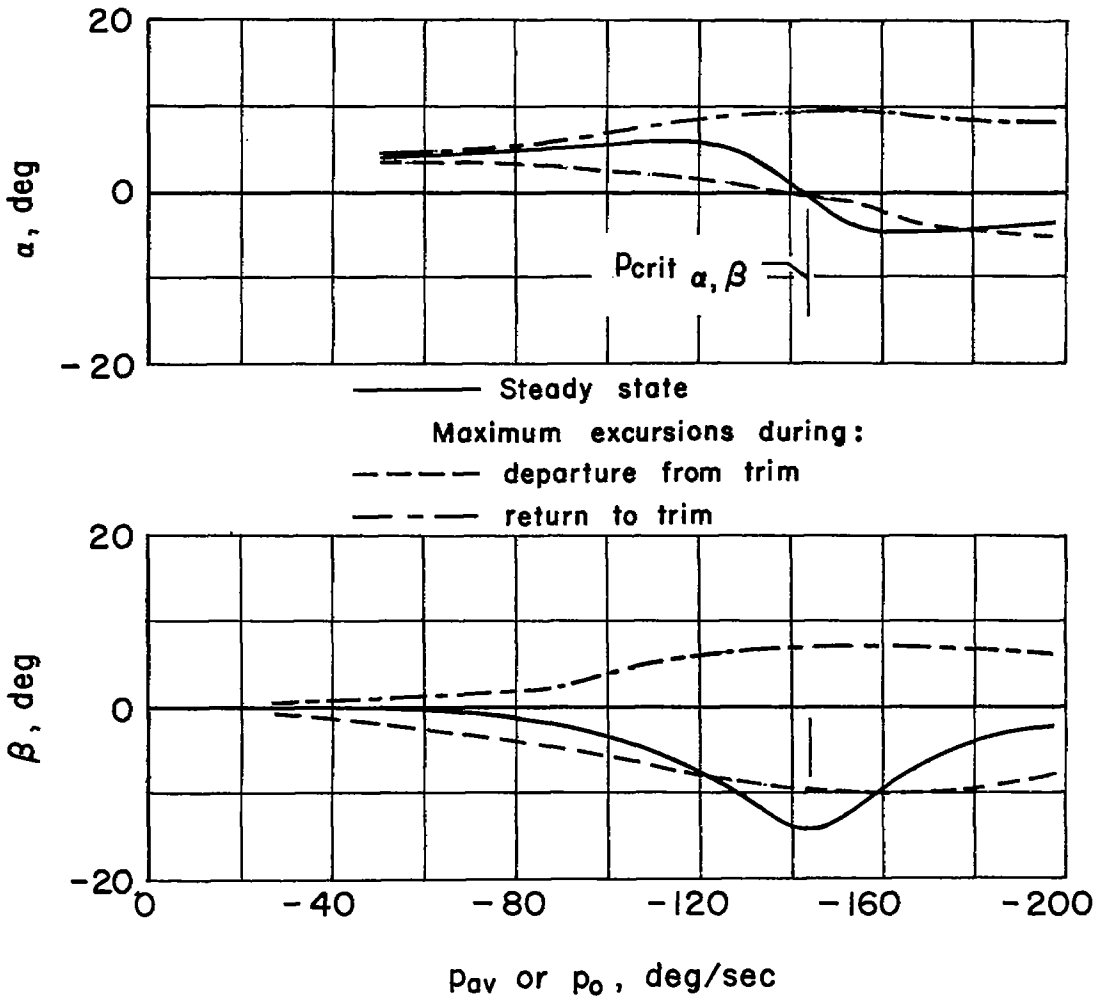

(a) $N_\beta = -M_\alpha \frac{I_3}{I_1}$; $M_\alpha = -6.74$

Figure 6.- Comparison of steady-state results with five-degree-of-freedom analog-computer results for different values of M_α and N_β.

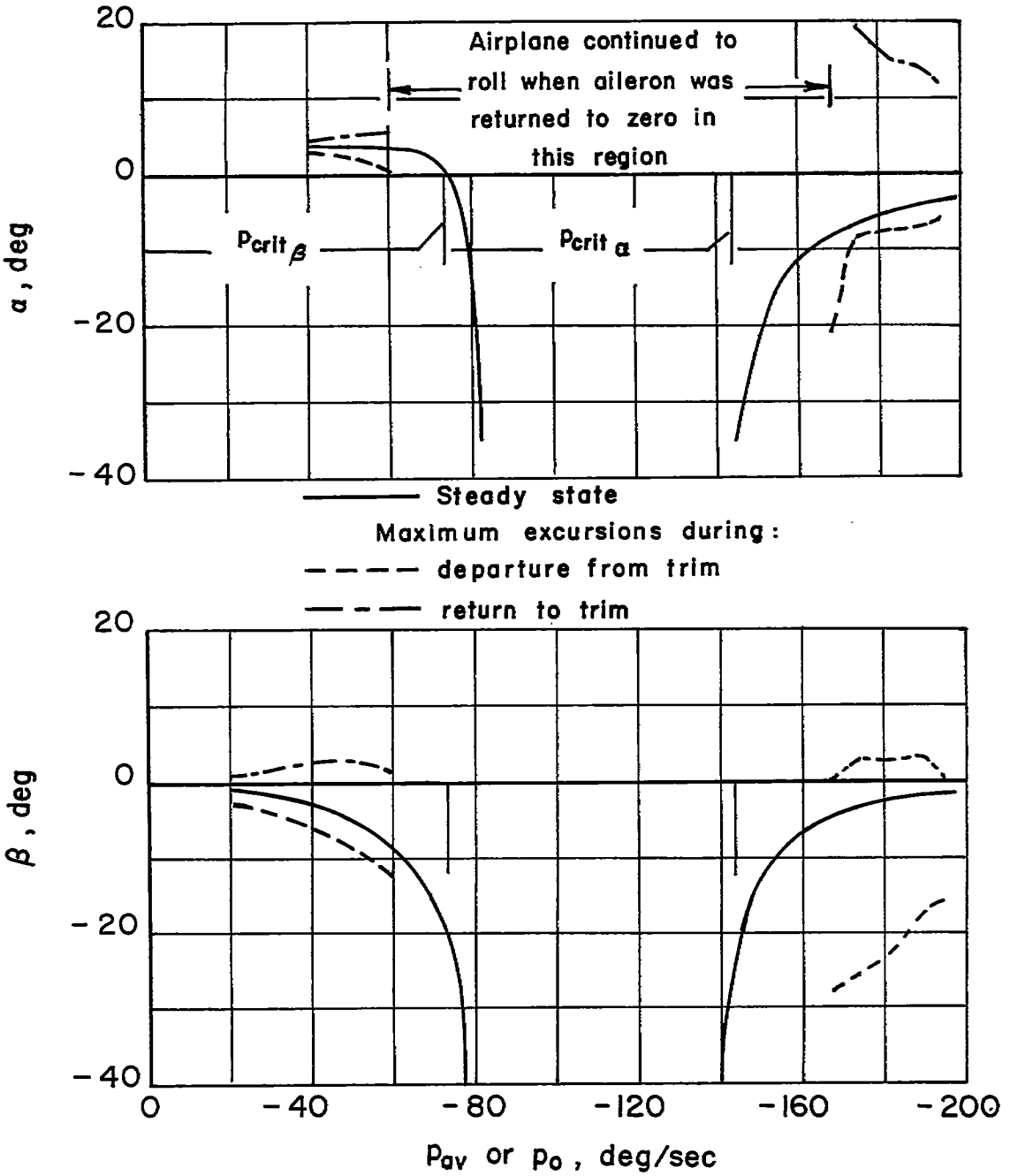

(b) $N_\beta = -0.3M_\alpha \frac{I_s}{I_1}$; $M_\alpha = -6.74$

Figure 6.- Continued.

[redacted]

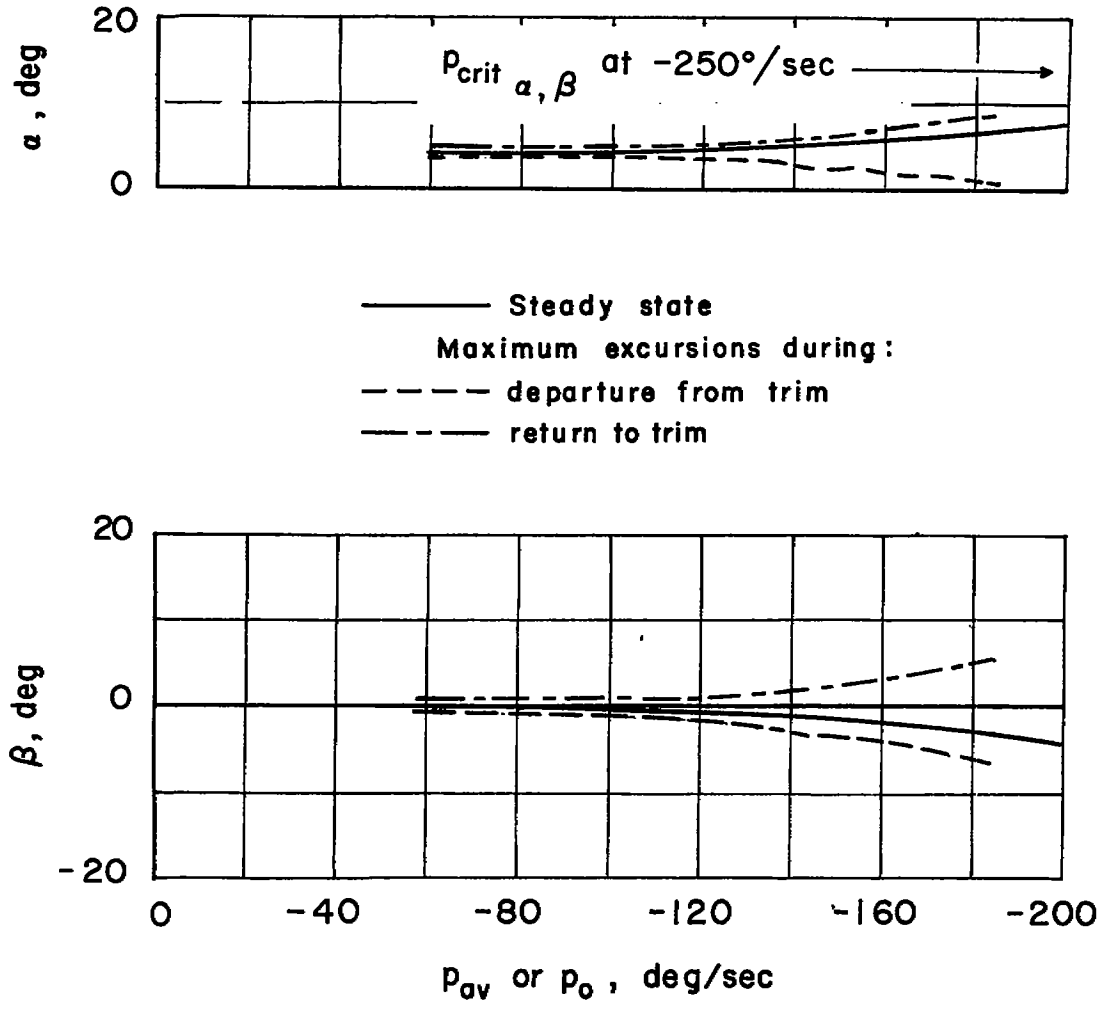

(c) $N_\beta = -M_\alpha \frac{I_3}{I_1}$; $M_\alpha = 3.0(-6.74)$

Figure 6.- Concluded.

[redacted]

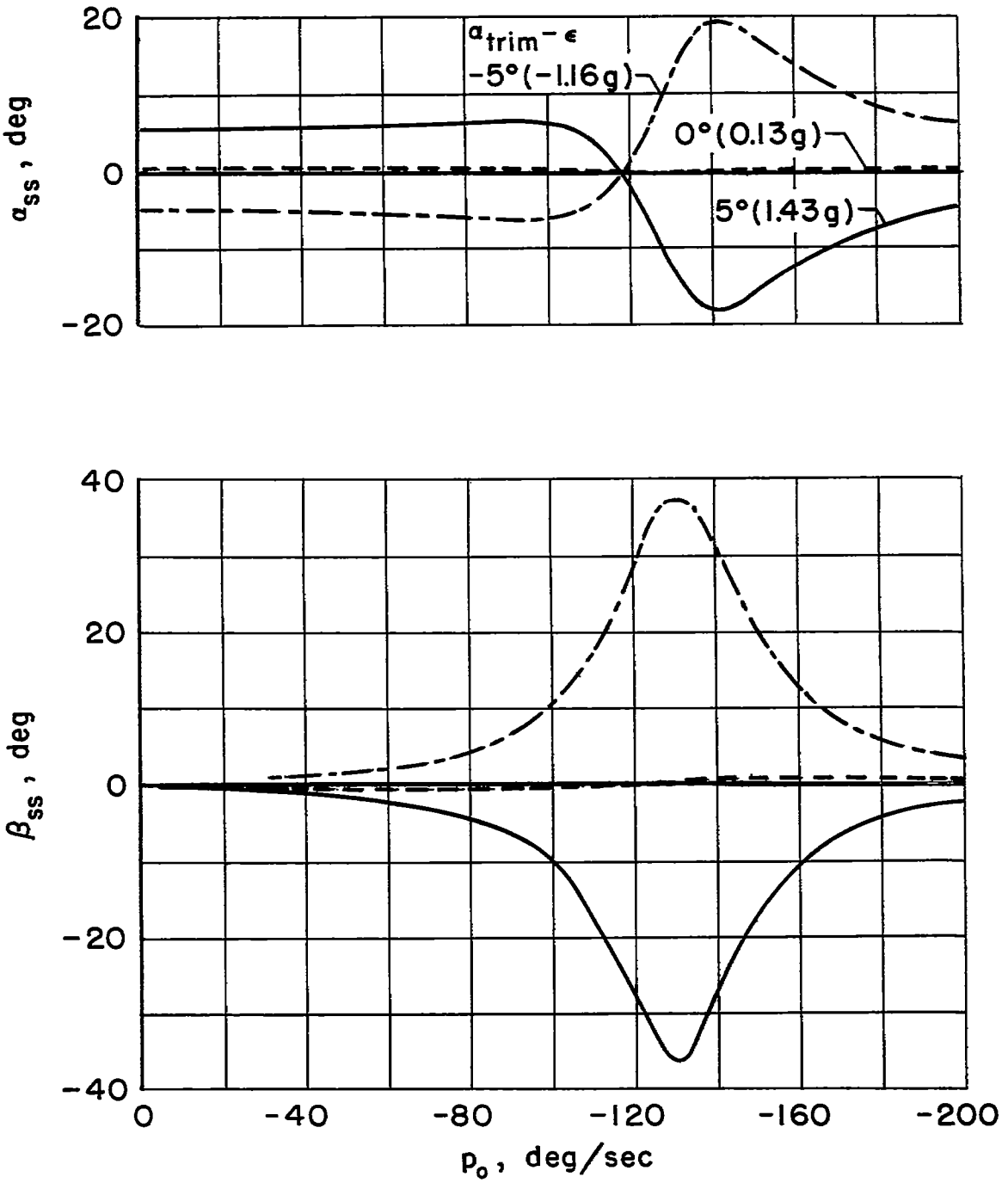

Figure 7.- Effect of nonalignment of principal and flight-path axes for the example aircraft using the simplified steady-state equations.

[redacted]

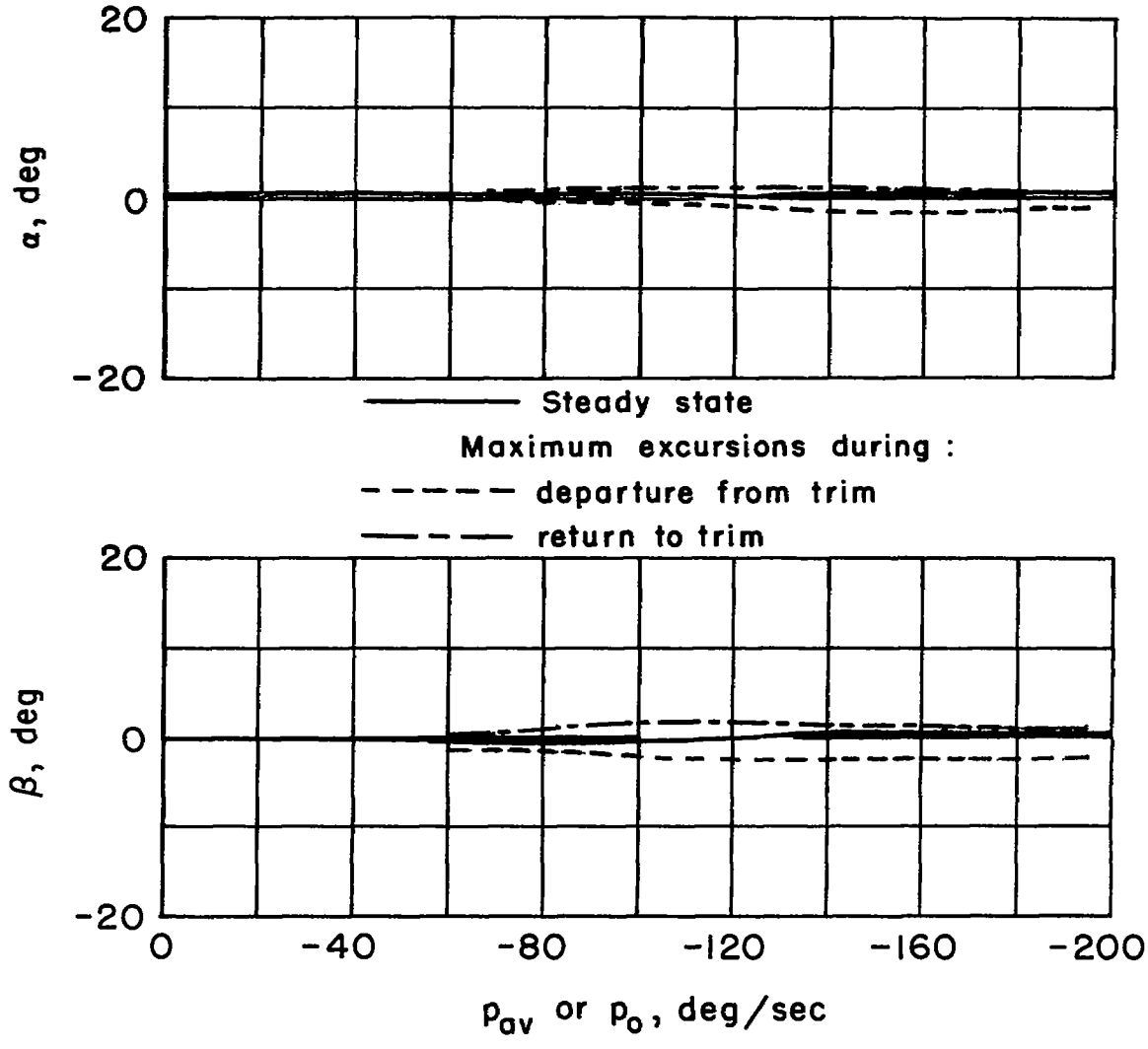

(a) $\alpha_{trim} - \epsilon = 0$

Figure 8.- Comparison of steady-state results with five-degree-of-freedom analog-computer results for the example aircraft with different alignments of principal and flight-path axes.

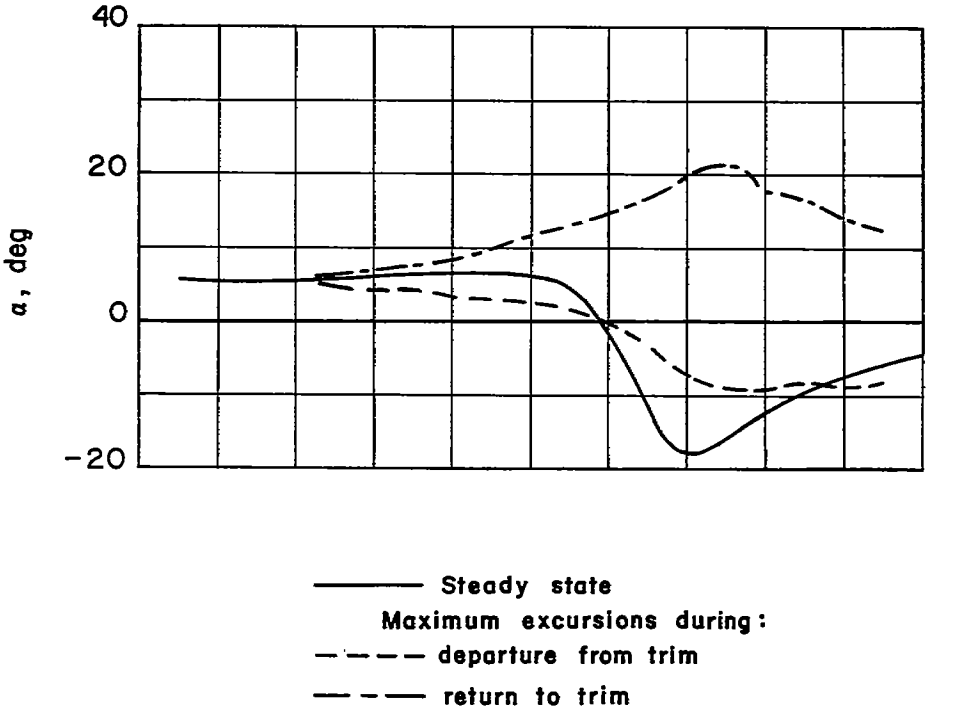

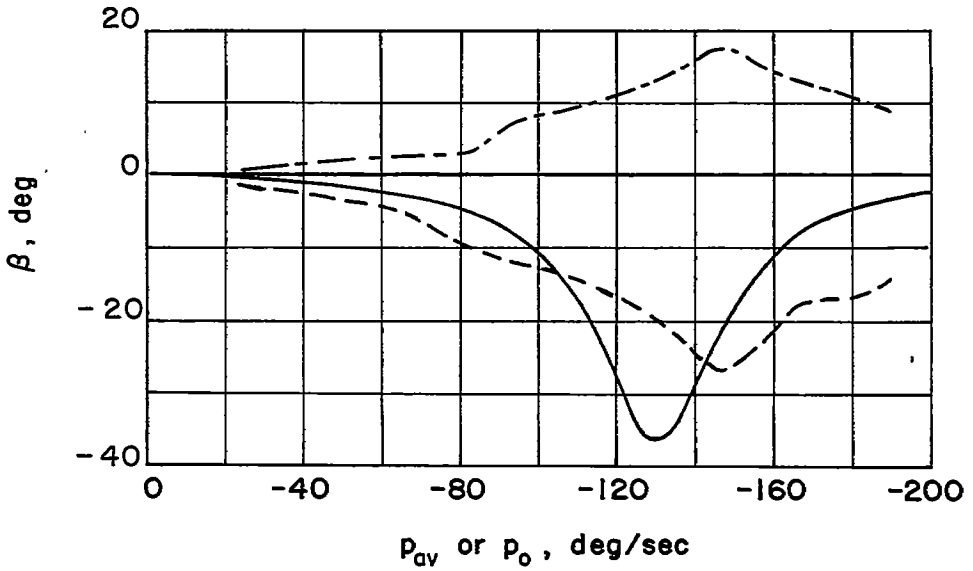

(b) $\alpha_{trim}-\epsilon = 5.0^{\circ}$

Figure 8.- Continued.

[redacted]

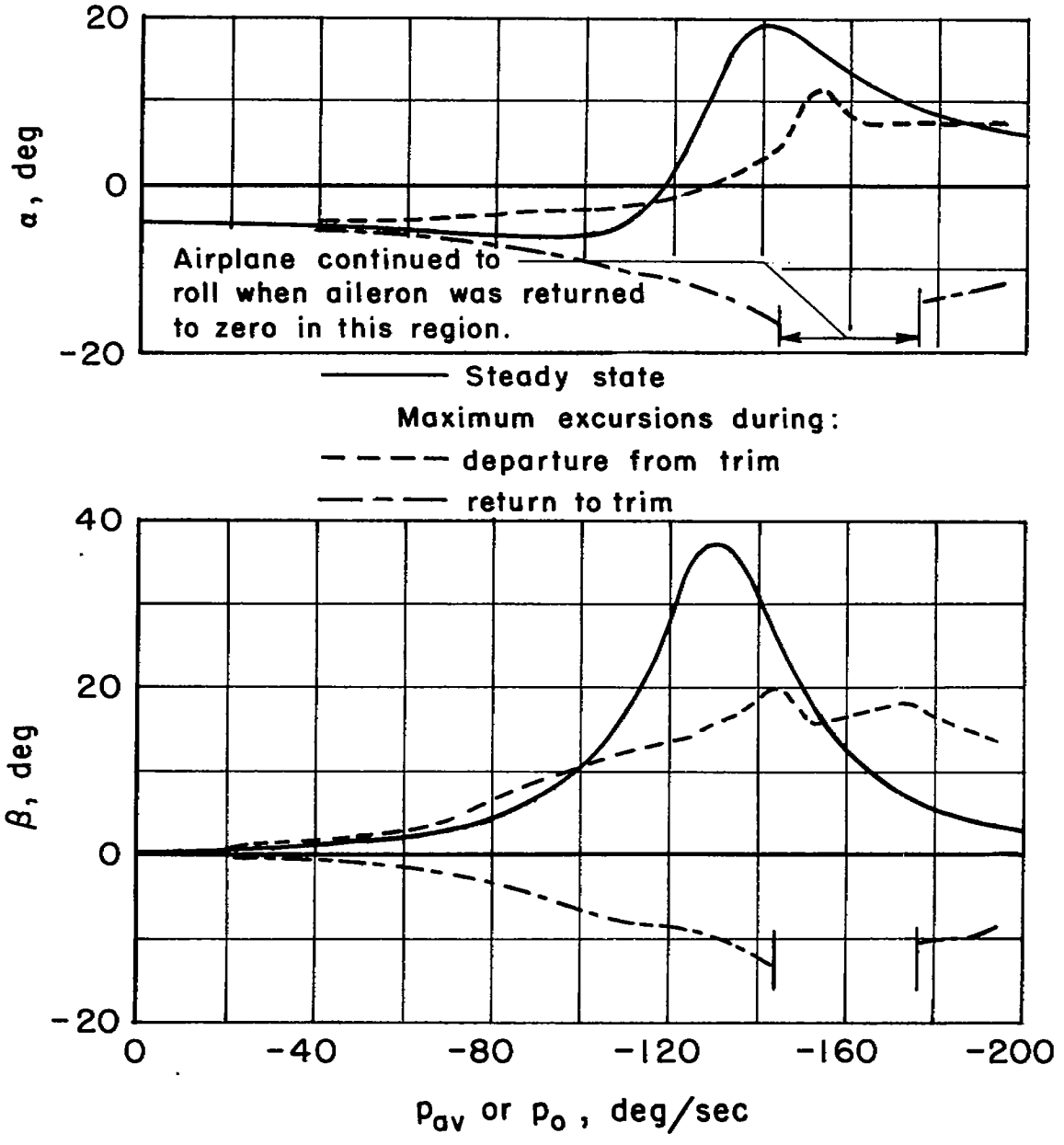

(c) $\alpha_{trim}-\epsilon = -5.0^{\circ}$

Figure 8.- Concluded.

[redacted]

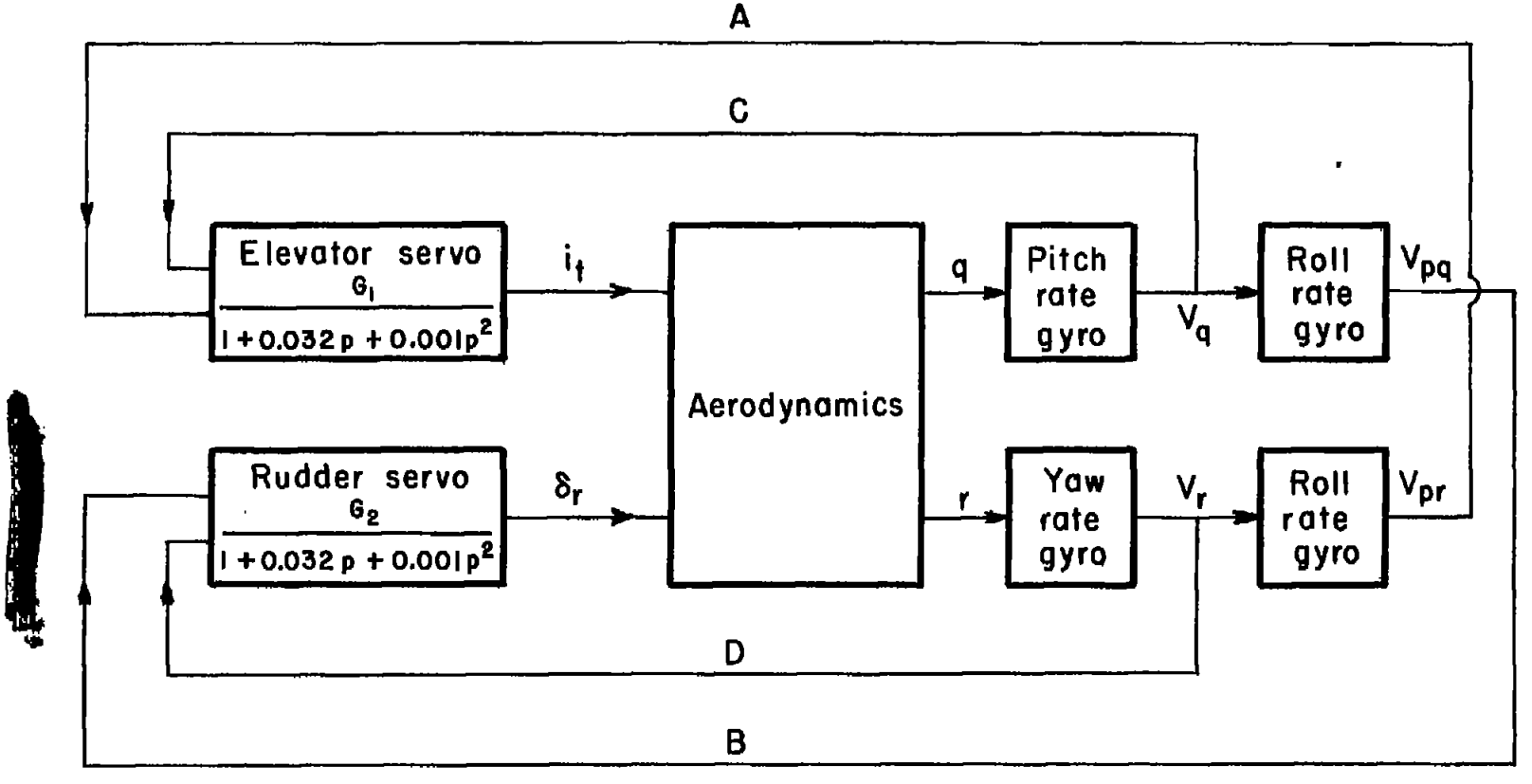

Figure 9.- Simplified block diagram of a stability augmenter incorporating damping and artificial nullification of inertia cross-coupling terms (pq,pr feedback).

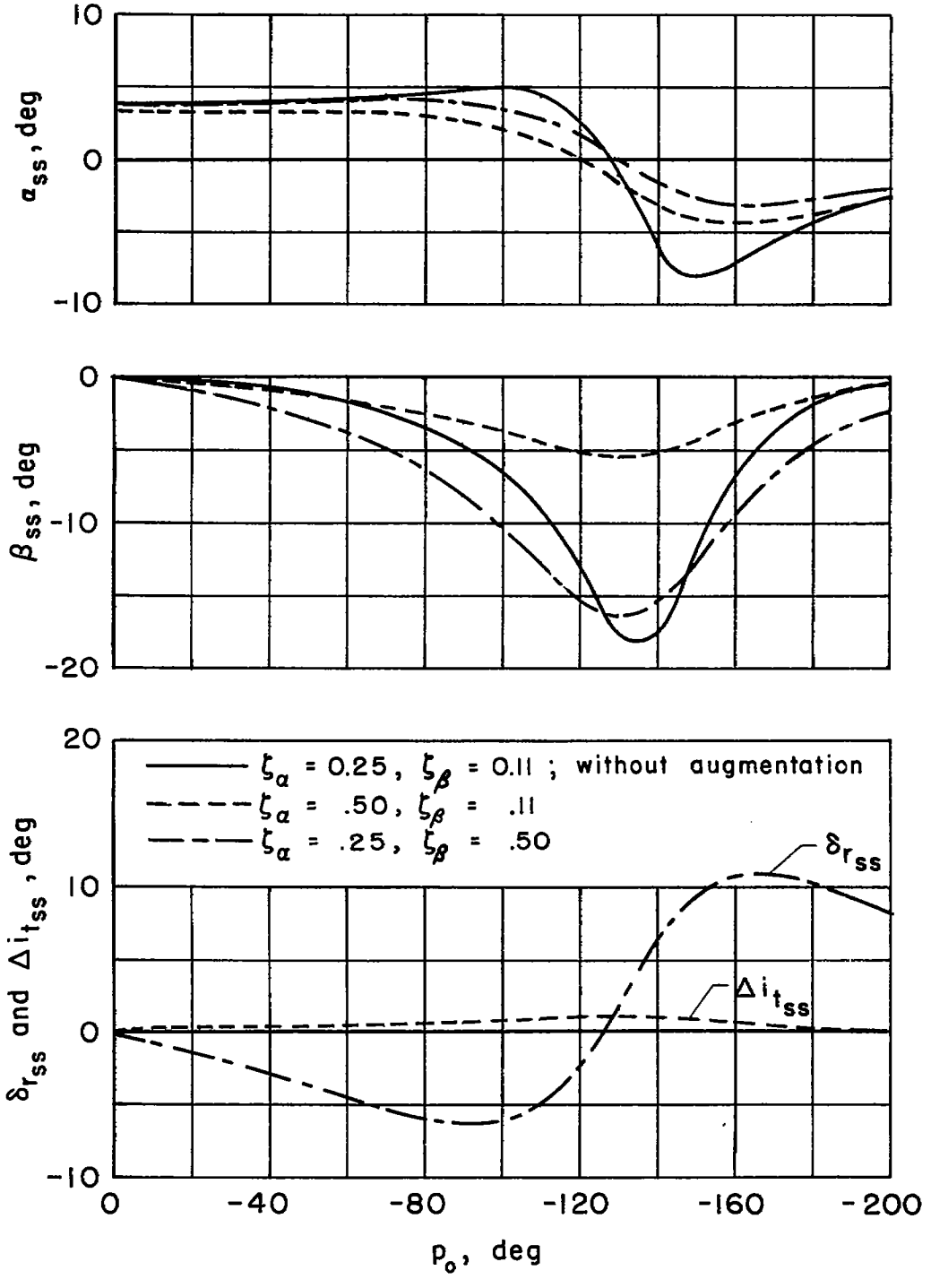

Figure 10.- Steady-state α, β, δ_r, and Δi_t for the example aircraft with different amounts of damping in pitch and yaw.

[redacted]

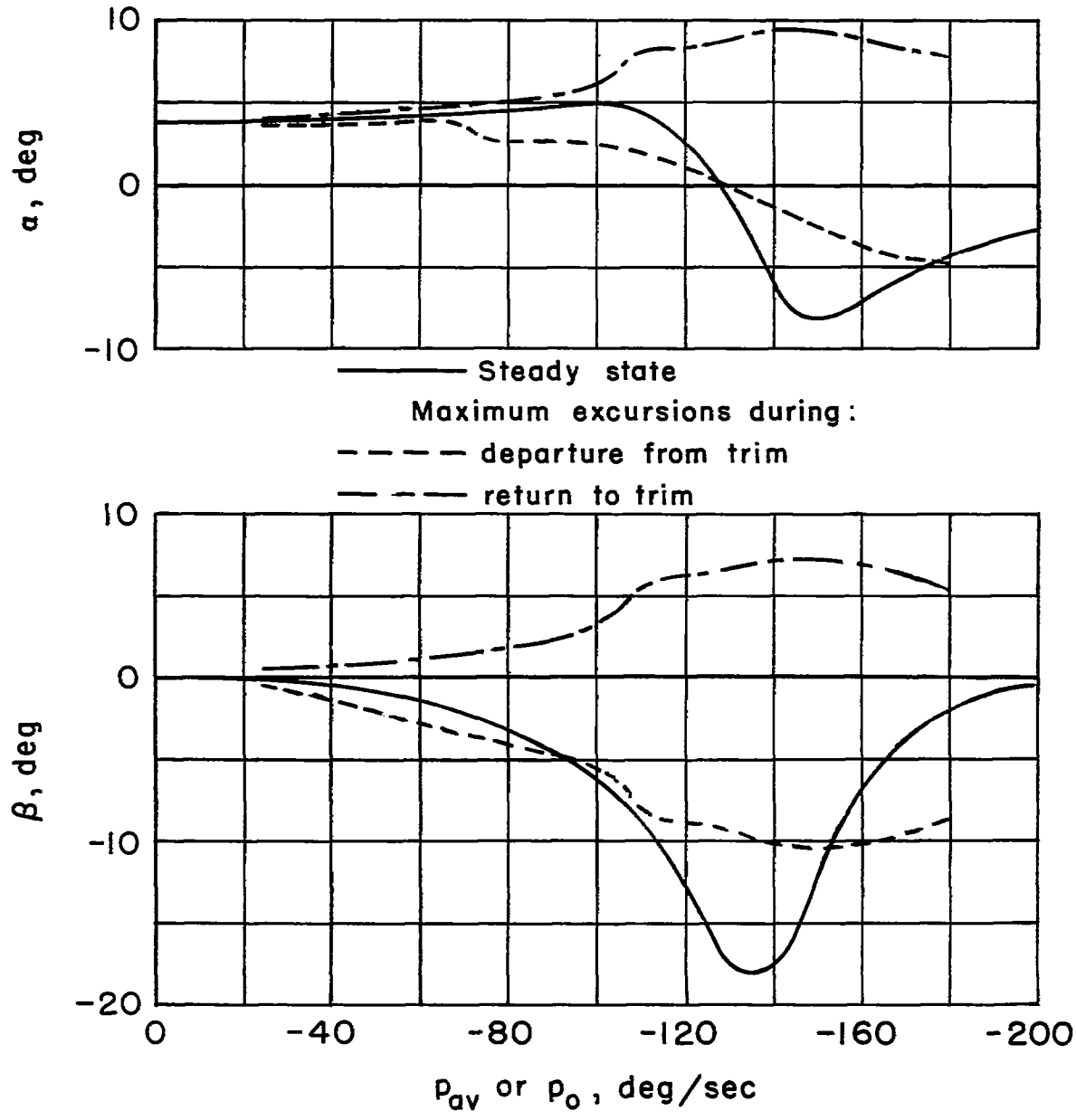

(a) Without augmentation; elevator and rudder fixed; $\zeta_\alpha = 0.25$; $\zeta_\beta = 0.11$.

Figure 11.- Comparison of steady-state results with five-degree-of-freedom analog-computer results for the example aircraft with different amounts of damping in pitch and yaw.

[redacted]

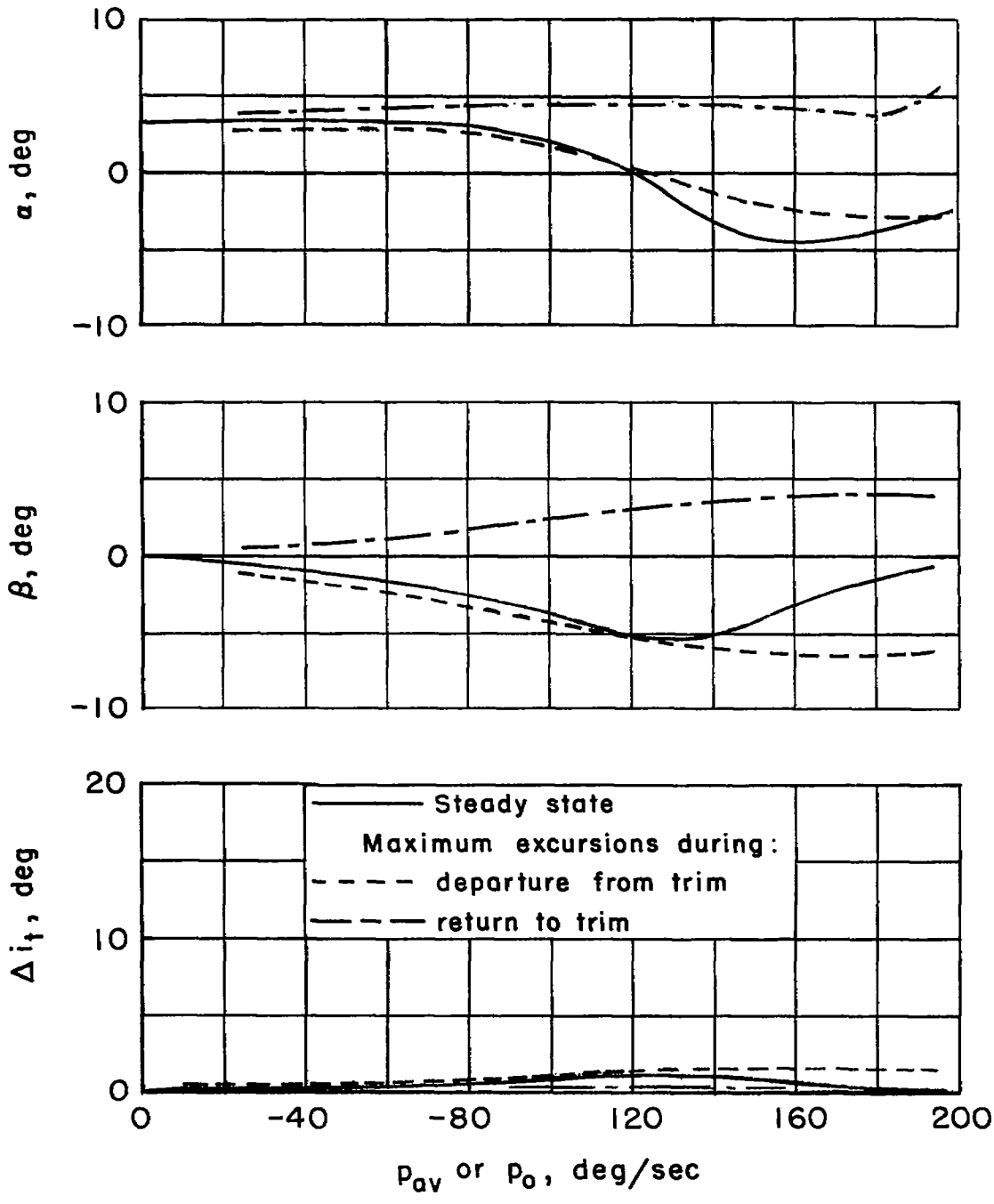

(b) Pitch damping increased to $\zeta_\alpha = 0.5$; $\zeta_\beta = 0.11$.

Figure 11.- Continued.

[redacted]

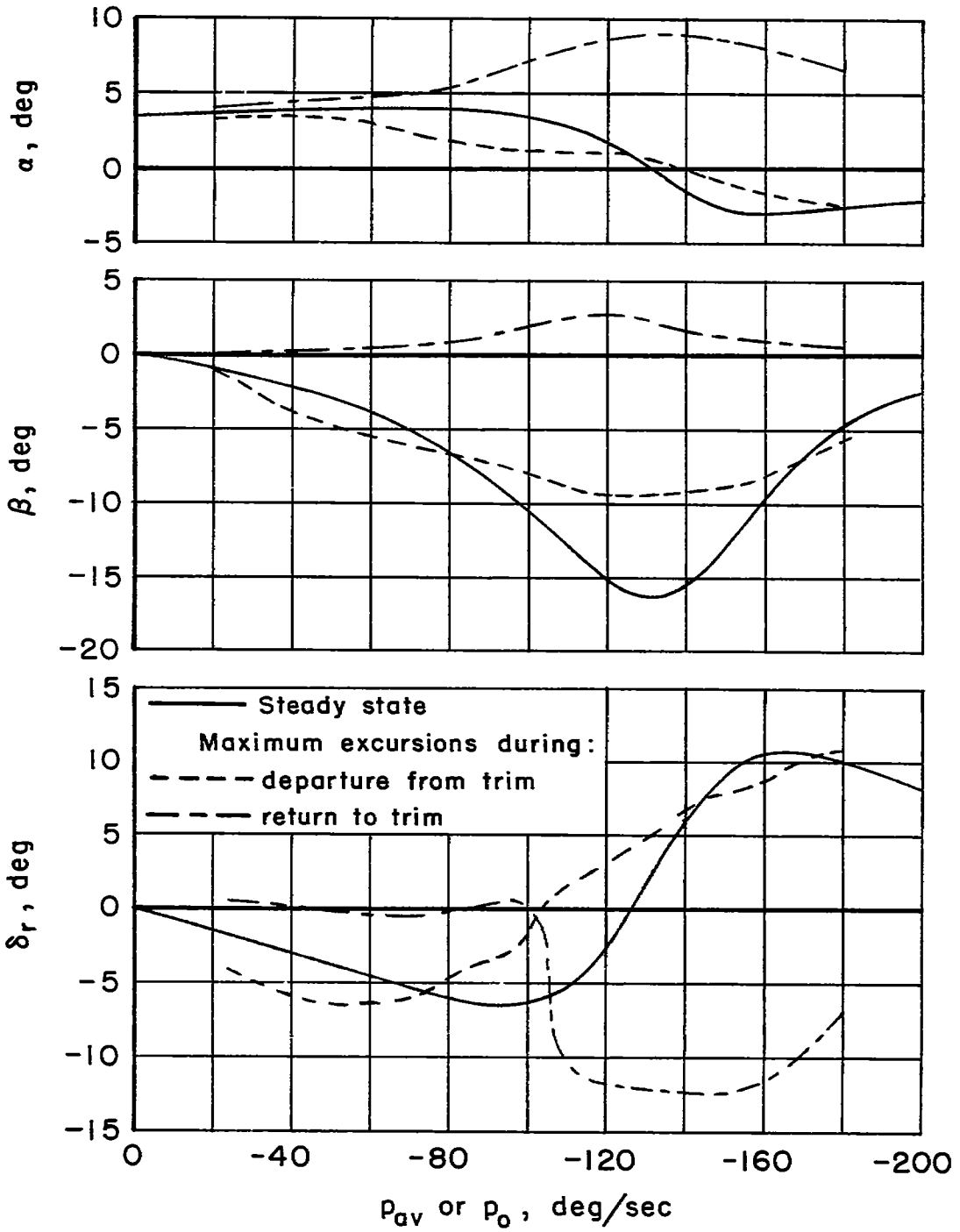

(c) Yaw damping increased to $\zeta_\beta = 0.5$; $\zeta_\alpha = 0.25$.

Figure 11.- Concluded.

[redacted]

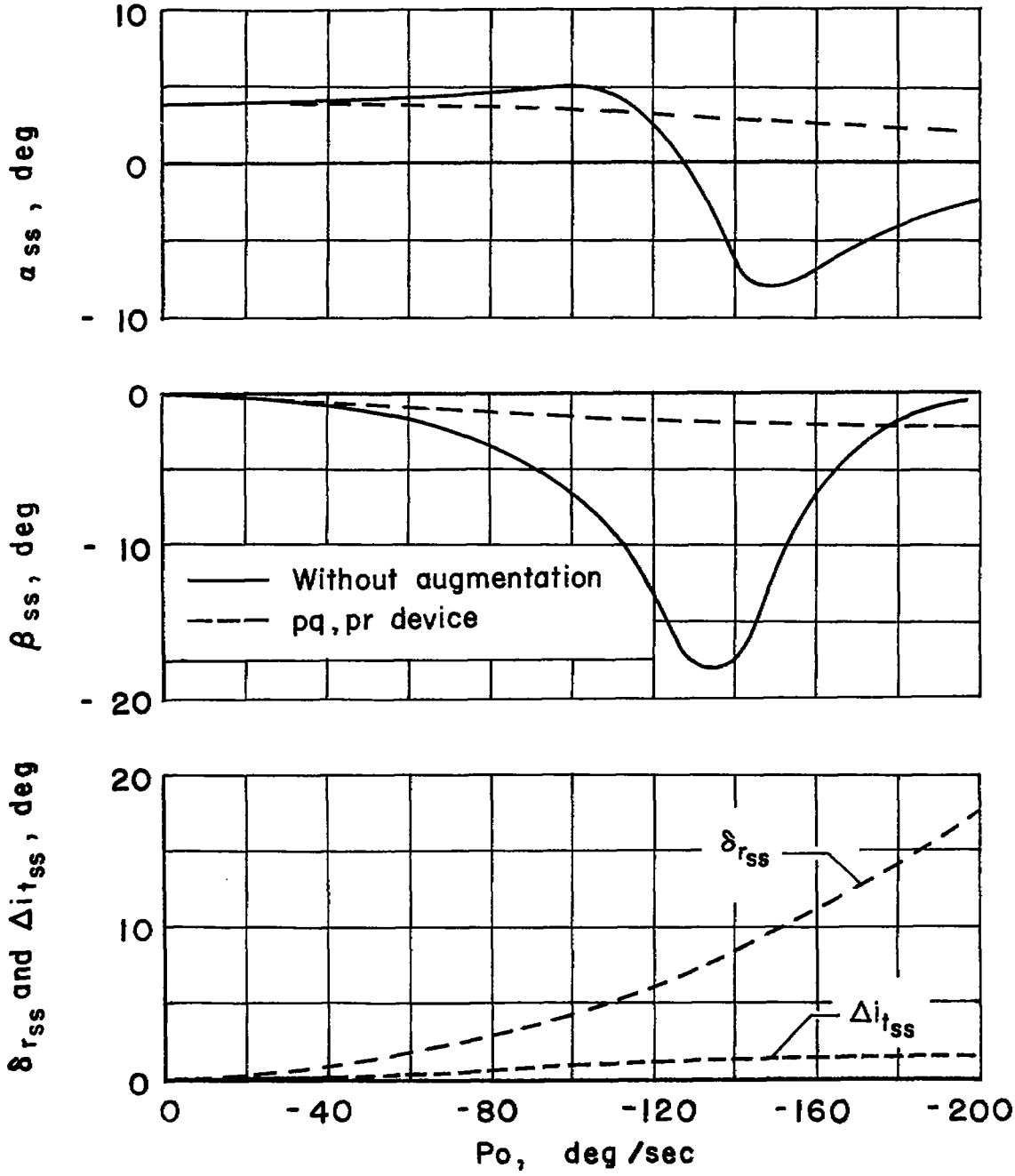

Figure 12.- Comparison of the steady-state response of the example aircraft with one augmented with a pq,pr device so that the inertia-coupling terms, $-I_1pr$ and I_3pq, are canceled.

[redacted]

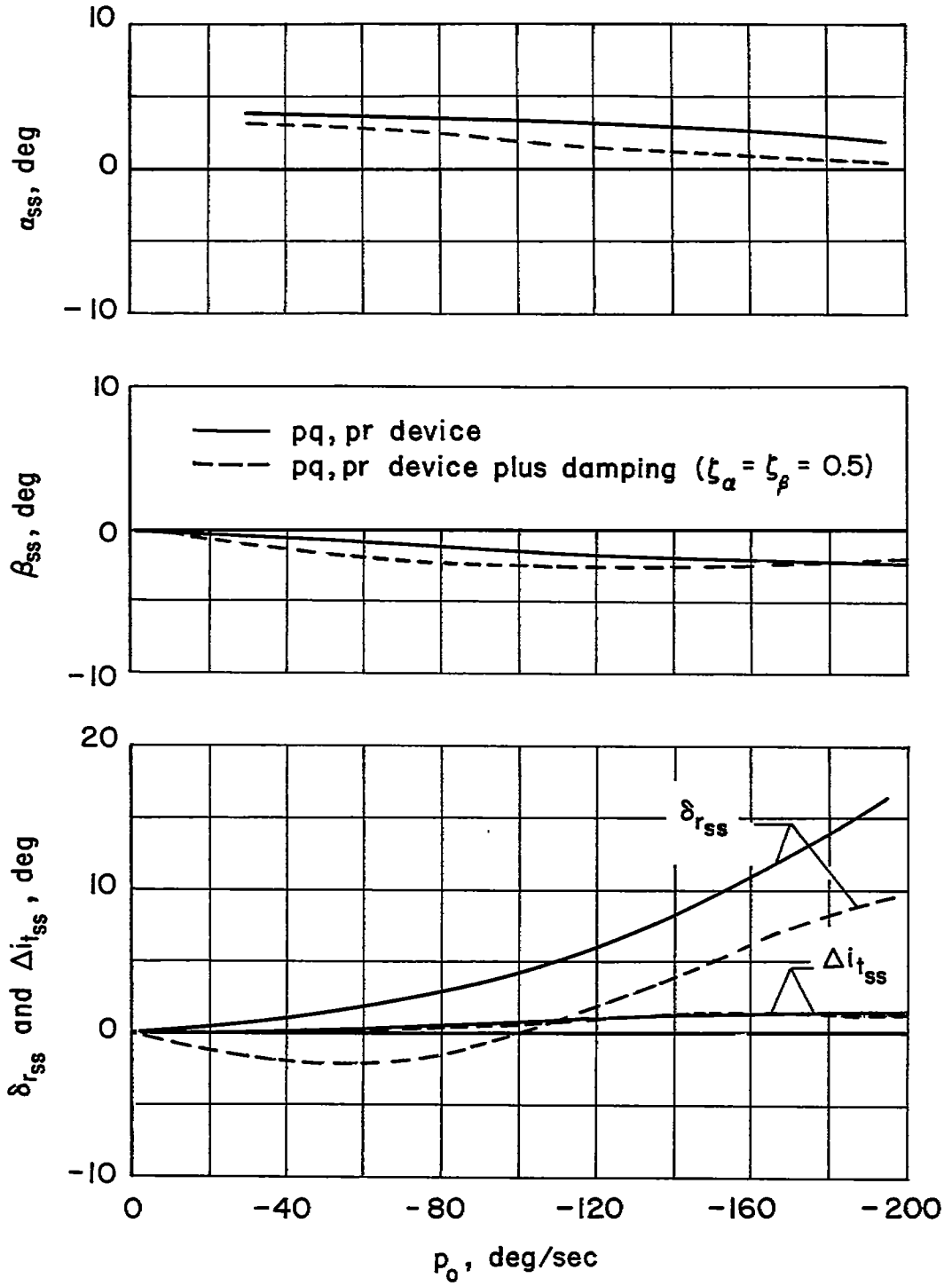

Figure 13.- Steady-state α, β, δ_r, and Δi_t responses for the example aircraft employing two types of stability augmenters.

[redacted]

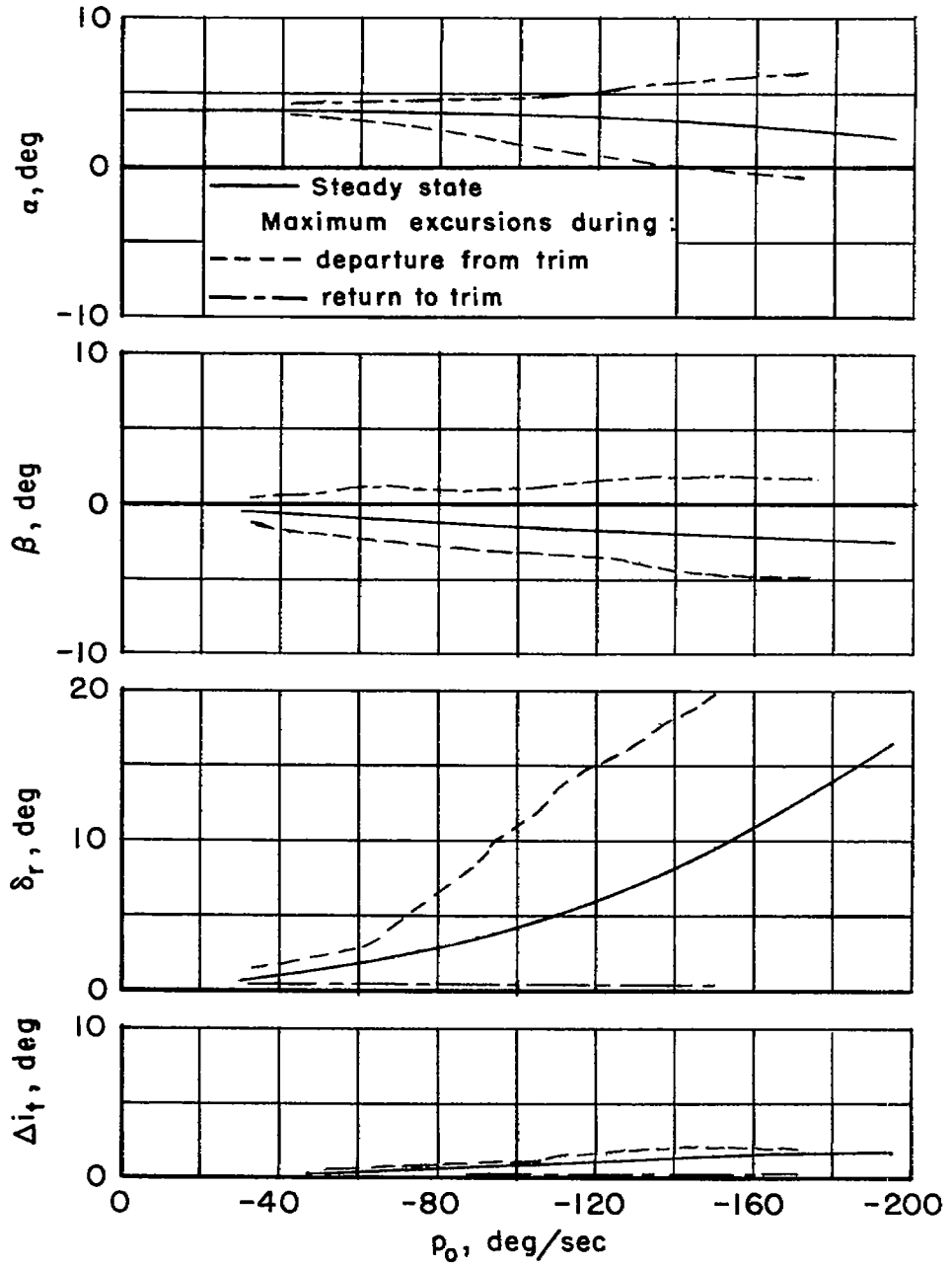

(a) The pq,pr device alone.

Figure 14.- Comparison of steady-state results with five-degree-of-freedom analog-computer results for the example aircraft with two types of stability augmenters.

[redacted]

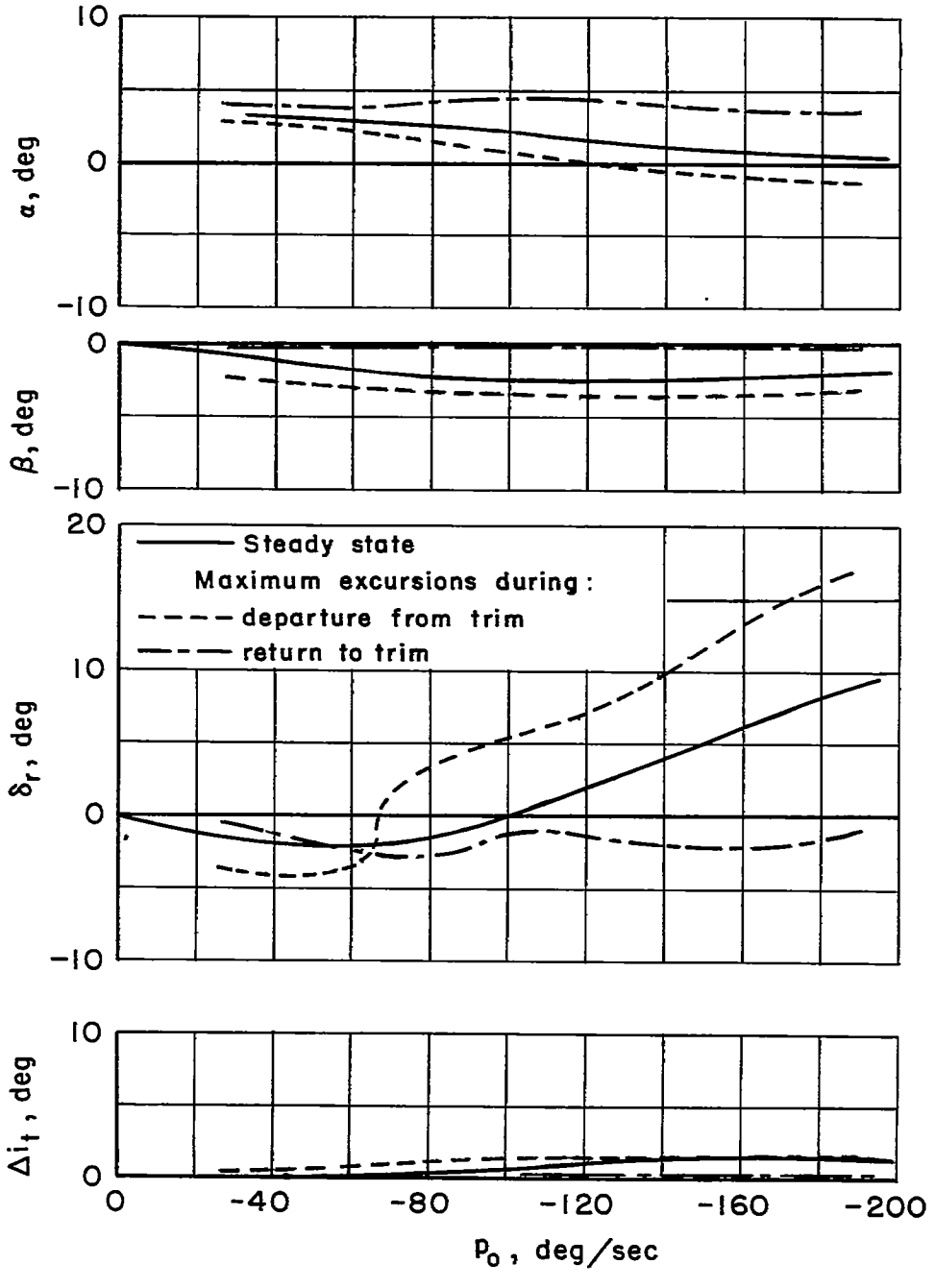

(b) The pq,pr device plus added damping; $\zeta_\alpha = \zeta_\beta = 0.5$.

Figure 14.- Concluded.

[redacted]

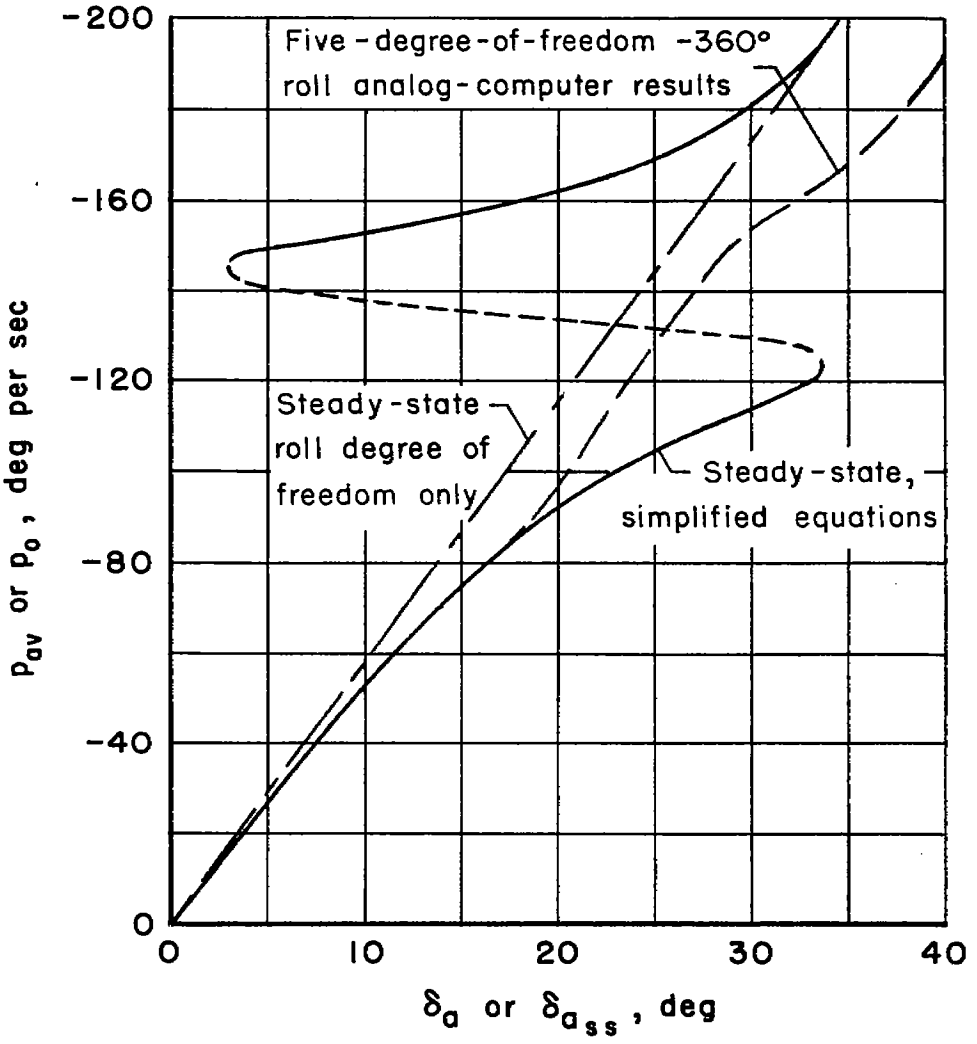

Figure 15.- Roll performance of example aircraft calculated by three different methods.

[redacted]

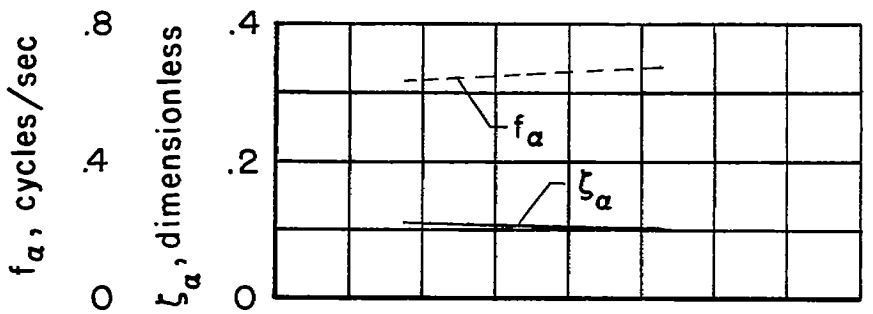

(a) Pitch mode.

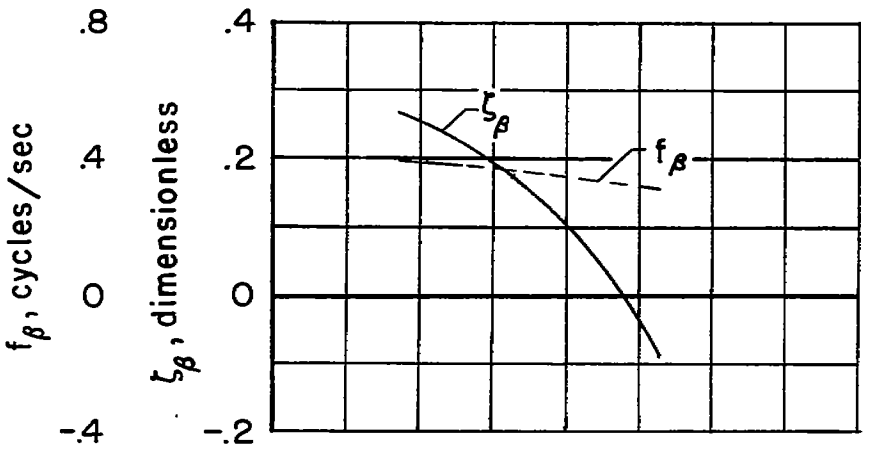

(b) Yaw mode.

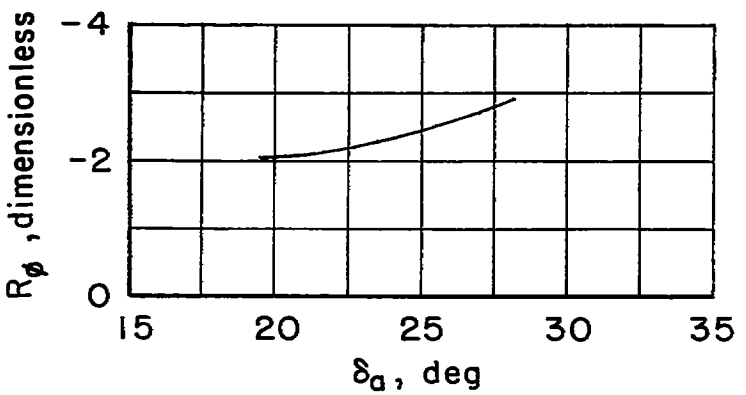

(c) Roll mode.

Figure 16.- Results of a perturbation analysis about the lower steady-state branch of the rolling performance curve for the example aircraft.

[redacted]

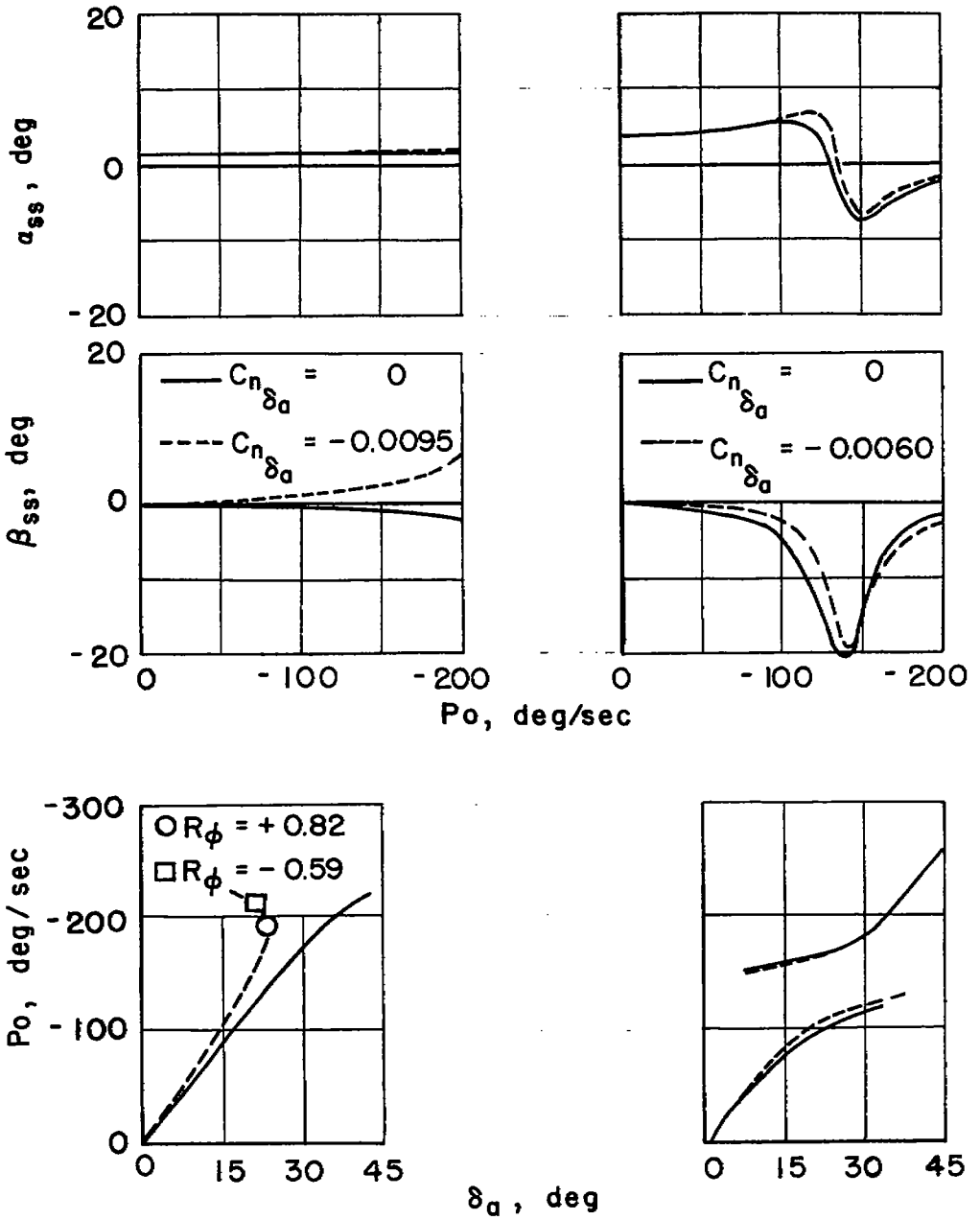

(a) Supersonic (M = 1.2). (b) Subsonic (M = 0.7).

Figure 17.- Variation of steady-state angles of attack, sideslip, and aileron deflection with roll rate as computed from the simplified equations showing the effects of the derivative $C_{n_{\delta_a}}$ for the large-tail F-100 airplane; h_p = 30,000 feet.

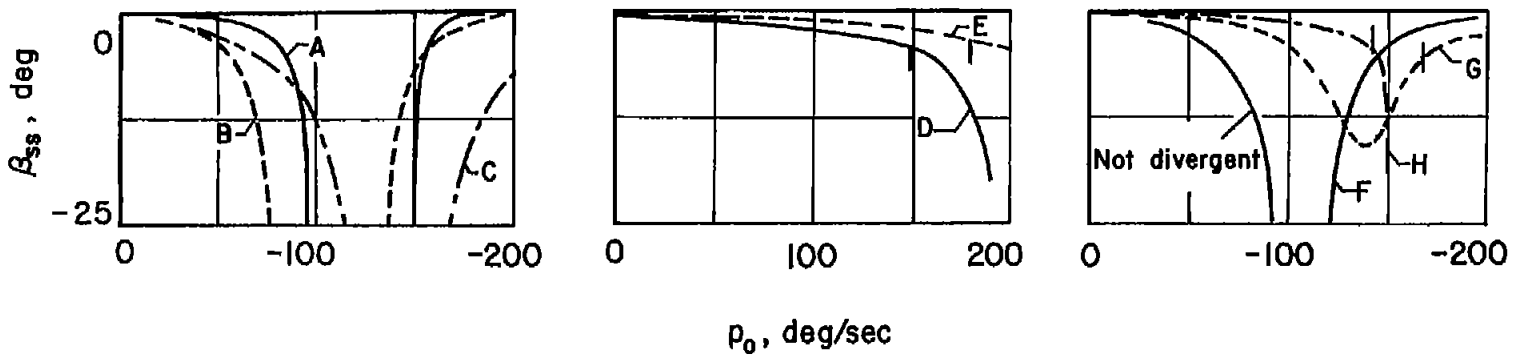

F-102 A

A M = 0.75 ; h_p = 39,500 ; 1 g

F - 100A, small tail

B M = 0.70 ; h_p = 32,000 ; 1 g

C M = 0.64 ; h_p = 10,000 ; 2.8 g

(a) Intolerable.

F - 100 A, large tail ; 1 g

D M = 1.26 ; h_p = 40,000 ft

E M = 1.20 ; h_p = 30,000 ft

(b) Good.

F - 100A, large tail ; 1 g

F M = 0.70; h_p = 40,000 ft

G M = 0.70; h_p = 30,000 ft

H M = 0.93; h_p = 40,000 ft

(c) Marginal.

Figure 18.- Comparison of steady-state solution with pilot opinion for several airplanes; 360° rudder-fixed aileron rolls.